Elucidating the mechanisms of action and evolutionary history of phage anti-defence proteins

Khalimat Murtazalieva[1,2], Evangelos Karatzas[1], Federico Corona[3], Jiawei Wang[1], Athanasios Typas[3] and Robert D. Finn[1#]

[1] European Molecular Biology Laboratory, European Bioinformatics Institute, Wellcome Genome Campus, Cambridge CB10 1SD, United Kingdom
[2] University of Cambridge, Cambridge CB2 1TN, UK
[3] European Molecular Biology Laboratory, Meyerhofstraße 1, 69117 Heidelberg, Germany
[#] Corresponding author: rdf@ebi.ac.uk

Highlights:

- The EVADES database aggregates knowledge on phage anti-defence proteins (ADPs), facilitating hypothesis generation.
- Mechanisms of action are proposed for 21 uncharacterised ADPs.
- ADPs that function as DNA mimics exhibit broad-spectrum activity, blocking or triggering diverse bacterial defence systems.
- Shared bacterial defence targets and functions underpin the multi-defence capabilities of ADPs and enable the prediction of additional targets.
- Eukaryotic double-stranded DNA viruses employ functional homologs of ADPs to evade host immune responses.

SUMMARY

Phages and bacteria are locked in a molecular arms race, with phage anti-defence proteins (ADPs) enabling them to evade bacterial immune systems. To streamline access to information on ADPs, we developed the Encyclopaedia of Viral Anti-DefencE Systems (EVADES), an online resource containing sequences, structures, protein family annotations, and mechanisms of action (MoA) for 257 ADPs. Through computational structural analysis we established putative MoAs for 21 uncharacterised ADPs. We demonstrate the utility of EVADES by exploring three hypotheses and demonstrate that: (i) ADPs acting as DNA mimics exhibit broad-spectrum activity against defences; (ii) protein sharing across defence systems enables multi-defence inhibitory activity of ADPs; and (iii) eukaryotic dsDNA viruses encode ADP homologs, suggesting conserved immune evasion strategies across domains. These results highlight the broader relevance of phage ADPs in understanding interactions between prokaryotic or eukaryotic viruses and their hosts. EVADES is freely accessible at https://www.ebi.ac.uk/finn-srv/evades.

KEYWORDS

phage-host interplay, phage anti-defence proteins, protein evolution, eukaryotic viruses

INTRODUCTION

Biological arms races—the adaptation between competing sets of co-evolving genes or organisms—are ubiquitous in nature. One such example is the perpetual arms race between bacteria and viruses, which has driven the evolution of bacterial defence systems that protect them against bacteriophage (hereafter termed phage) infections[1]. Currently known bacterial

defence systems employ a wide range of molecular mechanisms to prevent phage replication. These include degradation of phage nucleic acids, induction of abortive infection, or interference with essential molecular processes such as phage translation[1,2]. In response, phages have developed an array of anti-defence systems aimed at circumventing or neutralising these bacterial defences, thereby ensuring successful infection and replication[3].

Since the discovery of the first anti-defence proteins (ADPs) in the 1970s, the number of characterised systems has grown significantly[4], particularly over the past decade. This underscores the need for a resource that systematically classifies and describes ADPs to enhance our understanding of their mechanisms and evolutionary diversity. In this study, we compiled a comprehensive collection of ADPs, including their sequences, experimental or predicted secondary and tertiary structures, functional domains, and mechanisms of action (MoA). However, many entries have not been functionally characterised in terms of MoA, making it unclear whether they truly target defence systems or act via unrelated pathways that nevertheless yield positive assay results. Recognising this uncertainty, we incorporated Evidence Code Ontology (ECO) labels[5] to indicate the type of evidence supporting each entry, thereby improving transparency, interpretability, and confidence in the data. Complementing this, we conducted computational analyses and proposed putative MoAs for 21 previously uncharacterised ADPs, which we hope will help guide future experimental validation efforts.

Multitarget activity is an emerging functional theme among phage ADPs. Two striking examples of broadly acting ADPs are: (i) the T7 protein kinase[6], which exhibits anti-Retron-Eco9 and anti-DarTG1 activities; and (ii) the *Salmonella* phage JSS1 protein kinase[7], which exhibits activity against Dnd, CRISPR–Cas, QatABCD, SIR2+HerA and DUF4297+HerA systems. Both enzymes are promiscuous kinases that counteract multiple defence systems via phosphorylation. Another mechanism underpinning the multitarget activity of ADPs involves targeting conserved components or functions shared across distinct bacterial defence systems. Well-characterised examples include: (i) Thoeris anti-defence proteins 1 and 2 (Tad1/2)[8–10], which inhibit both Thoeris and CBASS systems by sequestering cyclic nucleotides; (ii) Ocr protein, which binds to PglX[11]—a core component of the Bacteriophage Exclusion (BREX) system—and also interacts with homologous HsdM methyltransferase in restriction-modification (RM) defence, thereby inhibiting both; (iii) S-adenosyl-methionine (SAM) lyase[12], which cleaves SAM, a molecule utilised by Restriction Modification (RM) and BREX defences, and exhibits anti-RM and anti-BREX activity; and (iv) NAD+ reconstitution pathways 1 and 2 (NARP1/2), which evade many defence systems that deplete NAD+, including Thoeris, DSR1, DSR2, SIR2-HerA, and SEFIR[13]. ORF58[14], with an uncharacterised MoA, evades Sir2+HerA and DUF4297+HerA defences, which share structural similarity[15]. We hypothesise that multipurpose ADPs may be widespread, as bacterial defence systems have evolved through tinkering—shuffling protein domains across different defence systems[16].

While compiling this database, it became evident that an increasing number of ADPs, while inhibiting one defence system, also activate another bacterial defence system[17–21], showcasing counter-counter adaptations. This activation may occur through direct interaction between bacterial defences and phage ADPs. For instance, the PARIS defence system forms a complex that binds the anti-BREX/RM protein Ocr from *Escherichia* phage T7, thereby releasing its toxic component, AriB, which cleaves lysine tRNA and triggers cell growth arrest[22]. This system can also be activated by the T4 Arn protein[22]. Likewise, the anti-RM protein Stp from phage T4 triggers the PrrC anticodon nuclease by binding the complex of PrrC with type I restriction enzyme EcoprrI[23]. Further supporting this model, the DNA mimic proteins Ocr and ArdA have

been shown to directly interact with and activate the self-guarded RM system EcoR22I, leading to programmed cell death, and to trigger the decoy system Ronin, which activates a membrane-disrupting toxin, RonA, in *Escherichia coli (E. coli)*[24]. Bacterial defences may recognise phage ADPs indirectly. For example, it has been proposed that the retrons Se72 and Ec48 "guard" the RecBCD system in *E. coli*, detecting the inhibition of the RecBCD complex —for instance, by phage *λ* Gam protein or the *T7* Gp5.9 protein—and triggering abortive infection[25]. Similarly, toxins associated with CRISPR–Cas systems play a comparable role, often inducing abortive infection when anti-CRISPR proteins (Acrs) inhibit CRISPR–Cas activity[26]. DNA methylases acting as anti-RM proteins can indirectly activate bacterial defence systems such as Dazbog, Nhi-like, and retron Sen2 by modifying bacterial DNA[20,25]. Supporting this, retron-Sen2 has been shown to contain a non-coding DNA molecule that is directly methylated by a phage DNA methylase [20]. Nevertheless, many mechanisms remain poorly understood—for example, how the anti-RexAB protein RIIB from phage *T4* activates the gasdermin defence[27] or how ORF58, an ADP active against Sir2+HerA and DUF4297+HerA, triggers Retron Ec86[14]. To better understand the properties of ADPs that trigger bacterial defence systems, we examined their features to identify common MoAs.

Finally, many components of eukaryotic immunity have evolved from bacterial defence systems[28,29]. For instance, nucleotide-binding oligomerization domain–like receptors (NLRs) of the STAND superfamily—ubiquitous pattern recognition receptors in eukaryotes involved in innate immunity—are homologous to the bacterial Avs-defence system, which recognises conserved viral proteins. Similarly, the eukaryotic cGAS–STING pathway, which senses double-stranded DNA (dsDNA) in the cytosol, utilises cyclic GMP–AMP synthase (cGAS)—a protein related to the CD-NTase (cGAS/DncV-like nucleotidyltransferase) employed in the bacterial CBASS (cyclic oligonucleotide–based antiphage signalling system) defence system. Moreover, evolutionary links between phages and eukaryotic dsDNA viruses have been extensively described[30–32]. For example, it has been hypothesised that polintoviruses were the first group of eukaryotic dsDNA viruses that evolved from bacteriophages, and that they subsequently gave rise to most large DNA viruses of eukaryotes[30]. This evolutionary history, together with reports of structural and catalytic active-site homology between the phage ADP Acb1 (which evades the CBASS defence system) and the poxvirus cGAMP phosphodiesterase (which inhibits the animal cGLR response)[33], led us to hypothesise that additional ADPs may be conserved between bacterial and eukaryotic viruses. Phage-encoded Thoeris anti-defence protein 4 (Tad4) and anti-CBASS protein 3 (Acb3) can inhibit innate immune systems in plants, animals, and humans—such as Toll/interleukin-1 receptors and cGAS—that are related to bacterial defence pathways[34], suggesting that retaining phage-evolved ADPs could be beneficial for eukaryotic viruses. We conducted a structure-based similarity search to identify similarities between phage ADPs and proteins in eukaryotic viruses. In this study, we focused on proteins that counteract defence systems shared between bacteria and eukaryotes to further investigate their evolutionary and functional relationships.

RESULTS

Diversity of phage ADPs

We have established the Encyclopaedia of Viral Anti-DefencE Systems (EVADES), which catalogues 257 ADPs that form components of 236 anti-defence systems[6–10,12–15,18,20,21,34–138], some of which are multicomponent systems (see Methods – Data Collection). Collectively, they target 40 families of bacterial defences. The EVADES database encapsulates a significantly broader diversity of phage ADPs compared to other resources (Figure 1A, Supplementary Table

1). For example, AntiDefenseFinder catalogues 176 ADPs across 156 systems[139]. The dbAPIS database describes 80 experimentally validated ADPs, along with their remote homologs[140]. In contrast, resources such as Anti-CRISPRdb[141,142], and AcrHub[143] focus exclusively on anti-CRISPR (Acr) proteins, with AcrHub containing 76 such proteins.

Beyond its broad range of ADPs entries, EVADES provides detailed MoAs, ECO labels, protein sequences, predicted and experimental structures, profile-hidden Markov models (HMMs), information on protein family membership and homologs in eukaryotic dsDNA viruses, and additional data—including the potential to trigger other defence systems. Only dbAPIS[140] and AcrHub[143] provide comprehensive information, but are restricted in their scope, while AntiDefenseFinder provides profile HMMs and protein sequences[139], but has fewer ADPs and lacks the breadth of information provided by EVADES.

We classified known ADPs into categories based on their MoAs (Figure 1B and Supplementary Figure 1): (i) ADPs with an unknown MoA (n = 104); (ii) ADPs that bind to bacterial defence components (n = 90), including 20 predicted in this study; (iii) ADPs that modify phage components to evade recognition (n = 15); (iv) ADPs that degrade or sequester signalling molecules/cofactors utilised by bacterial defences (n =13); (v) ADPs that synthesise or restore essential molecules depleted by bacterial defences, including one predicted in this study (n=10); (vi) ADPs that add covalent modifications to bacterial defence systems (n = 6); (vii) uncategorised ADPs (n = 6); and (viii) proteins that bind and protect components targeted by host defences (n = 4). While 69 out of 133 ADPs with experimentally characterised MoAs have known structures in the Protein Data Bank[144], the majority of uncharacterised ADPs (113 out of 124) lack structural data. To address this and gain insights into potential MoAs, we predicted protein structures for all ADPs lacking a known structure and performed structural similarity searches (see methods).

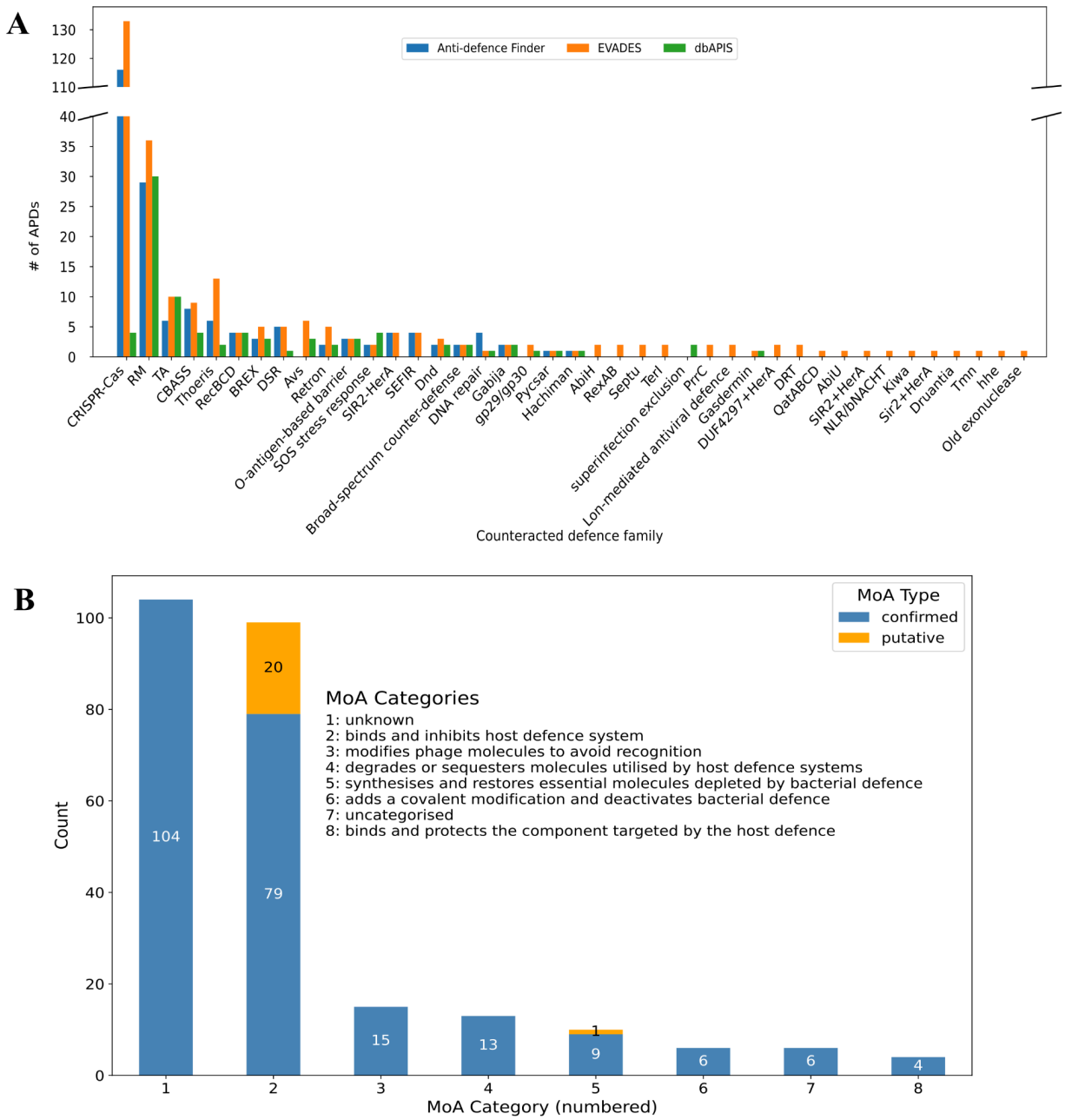

Figure 1. Overview of the database.

(A) Distribution of anti-defence proteins (ADPs) in AntiDefenseFinder (blue), EVADES (orange) and dbAPIS (green) by the family of targeted defence systems. The y-axis was truncated due to disproportionately high counts of anti-CRISPR proteins compared to other defence systems.

(B) Distribution of ADPs in EVADES. Bars represent the number of proteins assigned to each MoA category (1–8), with experimentally confirmed MoAs shown in blue and newly predicted ones from this study shown in orange. The total count for each category is displayed on the corresponding bar.

We also compared the sequences of ADPs to infer evolutionary relationships between them and found many pairs with high similarity at the sequence level (Supplementary Figure 2A). Interestingly, some of these pairs comprised proteins that counteract different defence families. For instance, Tad2[9] and AcrIIA7[51] shared high sequence and structure-based similarity (Supplementary Figure 2B-C, p-value = 2.55×10^{-8}). Tad2 sequesters gcADPR[9], a signalling molecule utilised by the Thoeris defence system. AcrIIA7 has been reported as type II-A anti-CRISPR protein with unknown MoA[51]. As type II CRISPR–Cas systems are not known to utilise cyclic signalling molecules, this similarity was unexpected. Although AcrIIA7 contains a variable central fragment that aligns poorly with Tad2, the rest of the sequence, including conserved residues, align well (Supplementary Figure 2C). Moreover, AcrIIA7 encodes residues similar to those at Tad2's active site. Based on these results, we concluded that AcrIIA7 is highly likely to sequester gcADPR, similar to Tad2 (Supplementary Figure 2B-C). During the course of this work, this functional prediction was validated by an experimental study[8]; however, the authors were unable to confirm the anti-CRISPR activity previously reported in a functional metagenomic screen[51]. Nevertheless, this example illustrates how structural computational biology approaches can elucidate molecular function based on similarity with other proteins. It also highlights the importance of including information on the nature of evidence supporting the anti-defence activity of database entries.

Inferring multi-defence activity of ADPs from defence protein-sharing network

Multi-defence activity is common among ADPs and is typically mediated by shared protein components across different defence systems. To explore this phenomenon further, we created a network based on structural similarity between bacterial defence proteins (represented as circular nodes) that either directly interact with ADPs or single-protein defences inhibited by ADPs with uncharacterised MoA, along with all other structurally related defence proteins (Supplementary Table 2). We then added ADPs as triangular nodes to indicate inhibitory interactions. The sharing of defence system components suggests that the inhibitory activity of ADPs may extend to the other defence systems that share similarity with those they are known to inhibit (Supplementary Figure 3A). For instance, it has been shown that Ocr binds to PglX, a component of the BREX defence system. PglX shares high similarity with gp28 from the Panchino defence, drmMI from Defense Island System Associated with Restriction-Modification (DISARM), and HsdM from the type I RM system. While inhibition of the type I RM system by Ocr has been demonstrated—specifically via binding between the HsdM and HsdR subunits—we hypothesised that Ocr may also inhibit DISARM and Panchino defence systems by binding to drmMI and gp28, respectively. This hypothesis is supported by AlphaFold 3 predictions of complexes between Ocr and drmMI or gp28. While these predictions are of moderate confidence, it is noteworthy that the binding interface of Ocr is similar in the two complexes (Supplementary Figure 3B).

20 ADPs with uncharacterised MoA are likely to acts as direct binders

Direct binders represent the most frequent characterised MoA category, leading us to hypothesise that some ADPs with uncharacterised function may also act via direct binding. To investigate this, we co-folded ADPs with uncharacterised MoAs alongside the proteins from the targeted defence systems (Supplementary Table 3). This analysis predicted 13 high-confidence interactions and 10 moderate-confidence interactions between ADPs and their corresponding defence systems (Supplementary Table 4).

While examining the results, we found that the complex between AcrIIA13 and *Staphylococcus aureus* Cas9 (*Sau*Cas9) had been confirmed by an almost identical structure (PDB accession: 7ENI). However, as this PDB entry lacked a corresponding publication, it had not been included in our database at that time. Additionally, we identified a recent paper (January 2025) that experimentally confirmed the interaction between Cas5e and AcrIE3—predicted by AlphaFold 3, with an interface predicted template modelling (ipTM) score of 0.84 and predicted template modelling (pTM) score of 0.84—but which had also not been included in our database[60]. We subsequently updated the MoA annotations for AcrIIA13 and AcrIE3, and added the other predictions, indicating that they are based on structural models.

We analysed our predictions alongside the original publications reporting ADPs to gain mechanistic insights and assess whether our predicted results align with available experimental data. For example, we predicted a high-confidence complex (ipTM = 0.92, pTM = 0.85) between AcrIC5 and *Pseudomonas aeruginosa* Cas8c (PaCas8c, NCBI GenPept accession: UEM35121.1). AcrIC5 has been reported to block *P. aeruginosa* CRISPR interference (CRISPRi), suggesting that it prevents target DNA binding[36]. Consistent with this, our prediction places AcrIC5 near the protospacer adjacent motif (PAM) binding site on PaCas8[145]. Notably, AcrIC5 is a highly acidic molecule (Figure 3A). The interaction between the PAM motif in the target DNA and the PAM-binding site on Cas proteins is essential for DNA binding. AcrIC5 may therefore displace the DNA and sterically block its binding. This prediction is consistent with the observation that AcrIC5 inhibits CRISPRi by preventing target DNA binding.

Another Acr reported in the same study, AcrIC3, did not inhibit CRISPRi, suggesting that it acts downstream of DNA binding[36]. The authors hypothesised that AcrIC3 could bind to Cas3 or Cascade in a manner that prevents Cas3 recruitment or DNA cleavage. We predicted a high-confidence (ipTM = 0.91, pTM = 0.90) interaction between the Cas3 endonuclease (GenBank: UEM35119.1)—spanning all four of its domains—and AcrIC3, supporting this conclusion (Figure 3B).

AcrIB4 is a puzzling example of an anti-CRISPR ADP, as it shares similarity to the C-terminal fragment of *Listeria seeligeri* Cas8b, raising the possibility that it may replace Cas8b during aberrant Cascade assembly. However, experiments have shown that AcrIB4 does not prevent the assembly of Cas8b or other core subunits (Cas7, Cas6, and Cas5) into the Cascade complex, and it has been reported to act upstream of target DNA binding [55]. The authors were unable to generate a functionally tagged version of AcrIB4 to directly assess its incorporation into the Cascade complex [55]. To understand the potential functional role of AcrIB4, we predicted a high-confidence interaction between AcrIB4 and LsCas8b (ipTM = 0.91, pTM = 0.76), specifically involving the C-terminal residues of Cas8b that mediate binding to Cas11 (Figure 3C). Cas11 is translated from an internal ribosome-binding site within the 3′ end of the *cas8b* gene and typically stabilises the non-target DNA strand during R-loop formation by positioning it above the crRNA–target DNA heteroduplex[146]. Based on this, we propose that AcrIB4 replaces Cas11 in the complex, thereby destabilising R-loop formation.

AcrIIA26 has been characterised as a potent inhibitor of *Streptococcus pyogenes* Cas9 (SpyCas9). It does not affect the formation of the Cas9–single guide RNA (sgRNA) complex but prevents this complex from binding to DNA, suggesting that it interferes at a downstream stage of the targeting process[37]. However, while AcrIIA26 was demonstrated to be an ADP, direct interaction between AcrIIA26 and SpyCas9 was not reported in that study. Consistent with the

experimental data, we predicted a high-confidence direct interaction (ipTM = 0.87, pTM = 0.79) between AcrIIA26 and SpyCas9, involving the negatively charged surface of AcrIIA26 and residues in SpyCas9 typically involved in target DNA binding (Figure 3D).

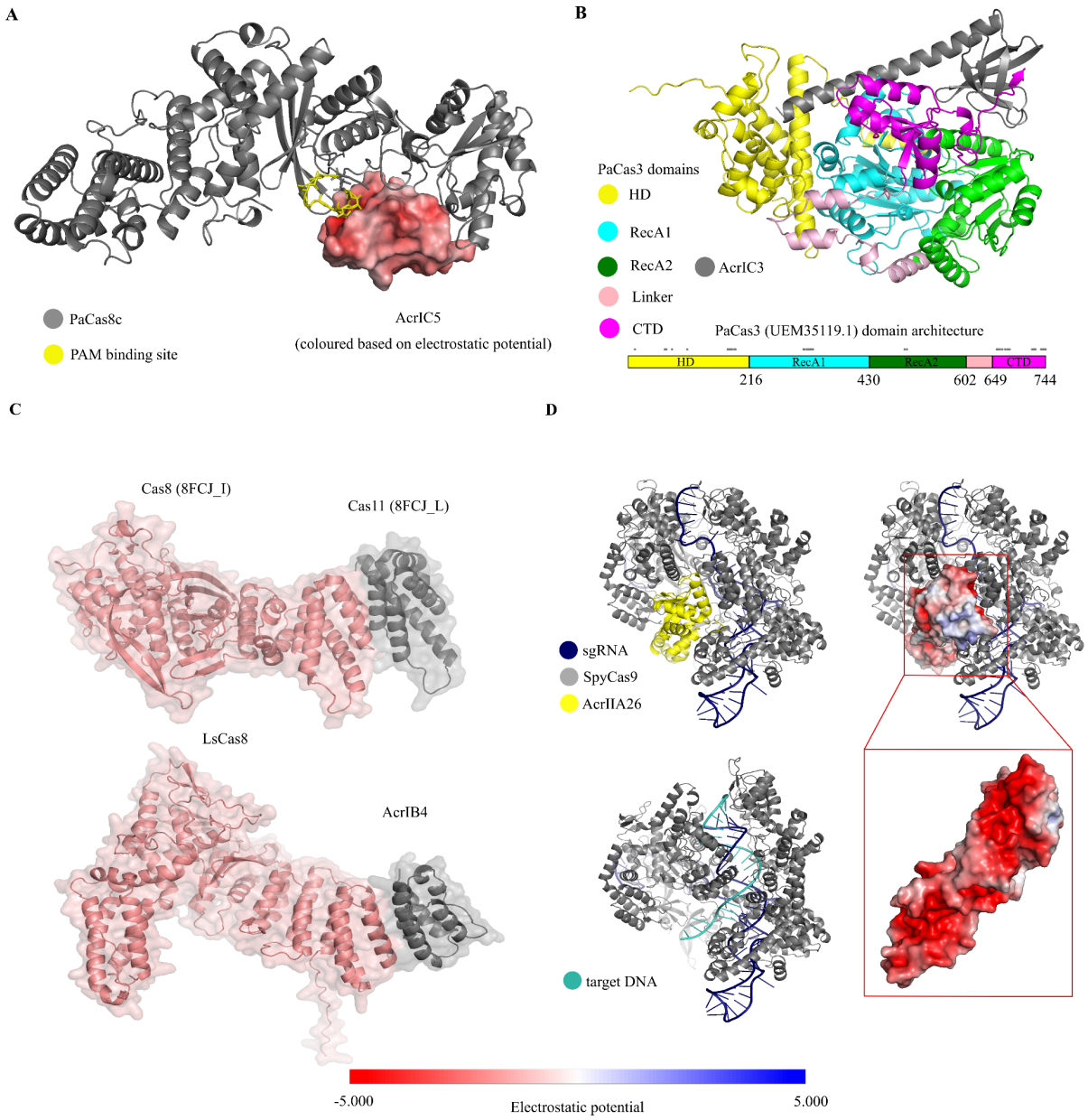

Figure 2. Putative mechanisms of action for ADPs based on structural model analysis

(A) AcrIC5 (surface rendered and coloured based on electrostatic potential) is a negatively charged protein that binds to Cas8c (grey, ribbon representations), occluding its protospacer adjacent motif (PAM)-binding site (yellow, side chains shown a sticks) and preventing Cas8c from interacting with the PAM site on the target DNA. **(B)** AcrIC3 (grey) binds to Cas3, with interactions spanning all four domains of Cas3: the HD nuclease (yellow), RecA1 (cyan), RecA2

(green), and C-terminal domain (CTD, magenta). Underneath the structure is a linear representation of Cas3 domain architecture, which is coloured as in the structure. Grey dots indicate the regions involved in interacting with AcrIC3. **(C)** Typically, the C-terminal domain of LsCas8b interacts with Cas11 (top), which stabilises Cas8 within the Cascade. AcrIB4 is likely to bind to Cas8b, replacing Cas11 in the Cascade. Cas8b from *Listeria seeligeri* (LsCas8b, coloured salmon pink) is predicted to bind AcrIB4 (grey) via its C-terminal domain (bottom).

(D) AcrIIA26 (yellow, top-left) is predicted to form a high-confidence complex with *Streptococcus pyogenes* Cas9 (SpyCas9, grey) and single guide RNA (cyan, sgRNA). The complex modelled between SpyCas9, sgRNA, and target DNA (cyan, bottom-left) suggests that AcrIIA26 is likely to occlude the SpyCas9's DNA-binding site. In the complex between SpyCas9, sgRNA, and AcrIIA26, the latter is coloured based on electrostatic potential (top-right). We rotated the view (using the commands "turn y, 135" and "turn x, 55") to show AcrIIA26's interface which interacts with SpyCas9 (bottom-right).

Phage ADPs trigger bacterial defence systems

The mechanisms by which bacterial defence systems sense phage infection remain poorly understood. However, several studies have identified the molecular triggers of these systems. Notably, Stokar-Avihail *et al.* conducted a systematic study aimed at uncovering phage determinants sensed by bacterial defences[25]. Their approach involved isolating phage mutants capable of escaping bacterial defences, sequencing them, and identifying mutations in either the protein-coding genes or in the intergenic regions adjacent to such genes. Such mutations were found in genes encoding structural proteins, components of the replication machinery, ADPs and proteins of unknown function. To extend this work, we compared entries in EVADES with those reported by Stokar-Avihail *et al.* to identify potential functions or relationships to newly discovered ADPs. We found that the Avs type I trigger from phage SBSphiC shares sequence similarity with *Bacillus* phage SP-10 deoxyuridylate (dUMP) hydroxymethylase, which is involved in genome hyper modification and protection from restriction enzymes[147]. We further searched for structural homologs of the type I Avs trigger in the PDB and found that it has extremely high similarity to cytidine monophosphate (CMP) hydroxymethylase MilA (Figure 3C, PDB: 5JNH; FATCAT 2.0 p-value =0.00e+00)[148]. However, there are indications that it may possess different substrate specificity from MilA. Zhao *et al.* reported that residues K133 and A176 determine MilA's specificity for CMP over dCMP, and mutations K133R and A176S shift its specificity towards dCMP[148]. Structural alignment of MilA with the Avs trigger revealed that R139 in the Avs trigger aligns with K133 in MilA and S183 aligns with A176 (Figure 3C). These observations suggest that the Avs trigger is more likely to function as a dCMP hydroxymethylase[25]—known to be involved in DNA hypermodification—rather than as a CMP hydroxymethylase. AlphaFold 3 also predicts a high-confidence complex between the type I Avs trigger and dUMP (ipTM = 0.97, pTM = 0.96), followed by a slightly lower confidence complexes with dCMP (ipTM = 0.94, pTM = 0.95) and CMP (ipTM = 0.92, pTM = 0.95). Overall, the results suggest that the type I Avs trigger is likely to act as an ADP involved in phage DNA hyper modification. Additionally, a mutation in an intergenic region upstream of gene 0.3 in T7 phage has been reported to enable escape from the retron Eco8 defence system[25]. Gene 0.3 encodes the anti-RM/BREX protein Ocr in T7 phages. This is a noteworthy observation, as Ocr has been reported to trigger the PARIS defence system via binding to AriA. AriA, along with the retron Eco8 effector protein, belong to the family of OLD nucleases[149,150]. It is therefore possible that

Ocr also triggers retron Eco8 through binding to its effector protein. However, structural modelling with AlphaFold 3 did not predict confident complexes between Ocr and the retron Eco8 effector, or between Ocr and AriA proteins from the PARIS defence system, despite experimentally verified direct interactions between AriA subunits and Ocr.

An analysis of phage genomes in RefSeq (see methods) revealed that phage ADPs reported to trigger bacterial defence systems have, on average, more homologs than other ADPs (Figure 3A, p-value 0.00129). These ADPs predominantly target bacterial systems that degrade nucleic acids and activate defences that induce abortive infection. This pattern may be explained by evolutionary dynamics: bacteria are more likely to develop new defence strategies against widely prevalent phage ADPs. By coupling an abortive-infection-inducing mechanism with one that degrades nucleic acids—should the latter fail to eliminate the phage—bacteria can maximise their protection while minimising collateral damage to their own population due to autoimmunity. Further supporting this interpretation, the expression of abortive infection (Abi)-inducing defence systems, such as Gabija and Nezha, has been shown to be negatively regulated by active CRISPR systems. Inhibition of CRISPR systems leads to the overexpression of these CRISPR-supervised immune systems (CRISIS), reinforcing the model of layered immune regulation[151].

Interestingly, five out of nine ADPs triggering bacterial defence systems are also DNA mimics. Given that there are 11 DNA mimic ADPs in the database (Supplementary table 5), this suggests that DNA mimics are significantly more likely to trigger bacterial defence systems (Fisher's exact test p-value 5.98×10^{-6}, Odds ratio 50.4), but acknowledge the total number is small. Nevertheless, we hypothesised that DNA mimics may bind a broad range of bacterial defence proteins that target nucleic acid[96], placing evolutionary pressure on bacteria to develop counter-counter adaptations—defence systems capable of recognising them. To investigate this, we co-folded DNA mimics with bacterial defence systems and predicted 20 high-confidence interactions (Supplementary Table 6), and 10 out of 20 of these interactions were with bacterial defence proteins binding DNA. We speculate that DNA mimics inhibit a broad range of DNA-binding defense systems and therefore exert strong evolutionary pressure on their hosts to evolve counter-counter-defense strategies that trigger abortive infection upon recognition of DNA mimics.

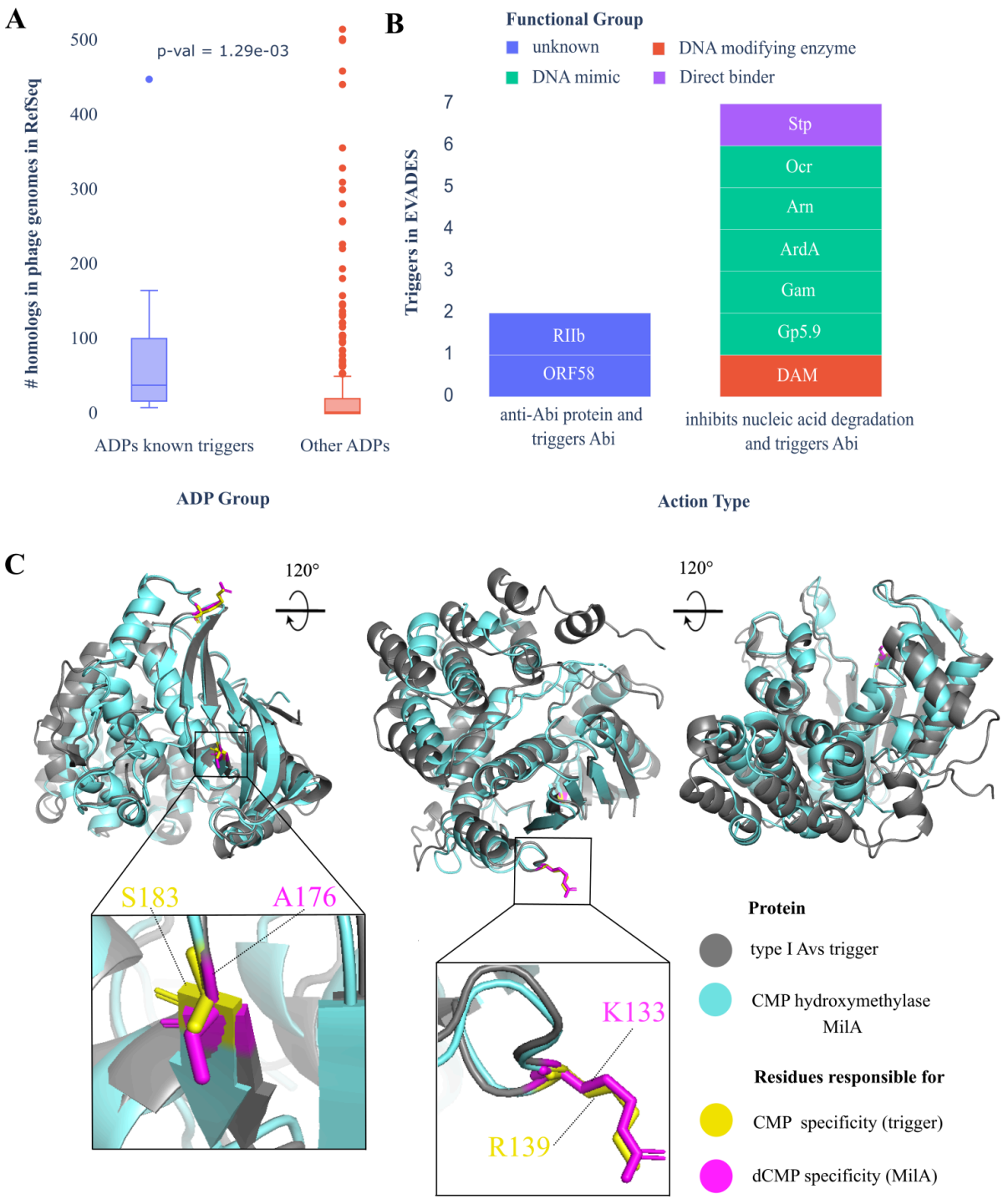

Figure 3. Phage ADPs trigger other defence systems.

(A) Boxplots showing the number of homologs of ADPs (those known to trigger bacterial defence systems [blue] vs. other ADPs [red]) in phage genomes from GenBank.

(B) Counts of ADPs found in EVADES that trigger other defence systems, organised based on the mechanism of action (Abortive Infection, Abi) and coloured by the functional group.

(C) Structural superposition of the Avs type I trigger from *Bacillus* phage SBSphiC (grey) and cytidine monophosphate hydroxymethylase MilA (cyan). Alignment was obtained with FATCAT 2.0 (p-value = 0.00e+00). Residues associated with CMP specificity are rendered as sticks and coloured in yellow, while those associated with dCMP specificity are in magenta and also rendered as sticks. The Avs type I trigger has substitutions likely responsible for dCMP specificity.

Eukaryotic viruses encode several homologs of phage ADPs

In order to assess conservation of defence evasion strategies between bacterial and eukaryotic viruses, we looked for structural homologs of phage ADPs in a database of 68K proteins encoded by eukaryotic viruses, including 43K proteins originating from dsDNA viruses[152]. We identified structural homologs for 23 ADPs, predominantly anti-RM proteins (n=10), followed by Acrs (n=3), anti-Avs (n=2) proteins, and anti-PrrC proteins (n=2). The two anti-PrrC proteins, which act sequentially in tRNA repair—a polynucleotide kinase and an RNA ligase—aligned with N- and C-terminal domains of the same eukaryotic viral protein, suggesting that both enzymatic activities are fused into a single multifunctional protein. Interestingly, several of these ADPs evade defence systems that are evolutionarily conserved between bacteria and eukaryotes[43,153,154,155]. For instance, the phage encoded ORF55 and ORF83 proteins evade the bacterial type III Avs (antiviral STAND) defence system[14], which shares homology with the STAND superfamily of pattern-recognition receptors involved in eukaryotic innate immunity[43]. Similarly, phage encoded nucleotidyltransferases (NTases) inhibit the STING pathway, a well-known immune signalling mechanism found in both bacteria and eukaryotes[50]. Another protein, Apyc1, antagonises the Pycsar defence system[46], components of which have homologs in eukaryotic genomes—raising the possibility that eukaryotes may possess a homologous signalling pathway[155,156].

Moreover, Schargel *et al.* have reported the presence of type II CRISPR-Cas homologs in eukaryotes[157]. However, the Acr proteins with homologs in eukaryotic viruses identified in our study target type I and VI CRISPR-Cas systems, which are distinct from type II. Therefore, it remains unclear whether these Acr homologs in eukaryotic viruses may play a role in immune evasion.

Anti-Avs ORF55 is a DNA ligase shared by bacterial and eukaryotic viruses

We next conducted a detailed analysis of these structural similarities to evaluate whether the underlying mechanisms of action are also shared between phage and eukaryotic viruses.

ORF55 is an anti-Avs type III protein identified in phage DruSM1 by Ojima *et al*[14]. Bacterial Avs systems detect phage-encoded proteins such as terminases and portal proteins, triggering homo-oligomerization and subsequent activation of the N-terminal effectors domains. Among these, DNA nucleases are the most prevalent effectors, inducing non-specific DNA cleavage upon activation. Interestingly, it has been demonstrated that bacterial Avs can also recognise portal proteins and terminase from eukaryotic viruses, including those from human herpesvirus 8[43].

ORF55 was annotated as an ATP-dependent DNA ligase[14]. Based on this annotation, we hypothesised that ORF55 may counteract the activity of the type III Avs effector proteins—non-specific dsDNA endonucleases [43]—by ligating DNA fragments cleaved during Avs activation. To investigate this possibility, we searched for structural homologs of ORF55 in the PDB. The closest match was identified as a Chlorella virus DNA ligase (PDB: 2Q2U, p-value = 0.00^{e+0})[158], a well-characterised enzyme involved in DNA damage repair[159](Figure 4A). This DNA ligase represents the minimal functional unit of the ATP-dependent DNA ligases and exhibits intrinsic nick-sensing activity, binding with high affinity to duplex DNA containing a single 3′-OH–5′-PO4 nick[160].

Structural alignment revealed that ORF55 retains 11 out of 13 active site residues conserved in the Chlorella virus DNA ligase (Figure 4B). We used AlphaFold 3 to model the structure of ORF55 in the complex with the DNA fragment co-crystallised with the Chlorella virus DNA ligase, which produced a high-confidence complex (ipTM 0.88, pTM = 0.91) with a similar DNA binding interface (Figure 4A).

Given that the Chlorella virus ligase efficiently ligates nicked DNA, performs poorly on one-nucleotide gaps, and fails entirely on two-nucleotide gaps[160], we modelled three complexes: ORF55 with ATP and (i) nicked DNA, (ii) one-nucleotide gapped DNA, and (iii) two-nucleotide gapped DNA. AlphaFold 3 predicted very high confidence for the nicked (ipTM = 0.95, pTM = 0.95) and one-nucleotide gapped complexes (ipTM = 0.95, pTM = 0.95), but lower confidence for the two-nucleotide gapped complex (ipTM = 0.87, pTM = 0.91). These results suggest that ORF55 from the DruSM1 phage shares a similar substrate preferences to the Chlorella virus DNA ligase, favouring nicked and one-nucleotide gapped DNA.

We identified homologs of ORF55 in 66 different species of eukaryotic dsDNA viruses infecting a wide range of hosts, including amoebae, algae, insects, invertebrates, birds, and mammals—most notably humans. The ORF55 homologs that have been functionally characterised and are involved in DNA repair, for example, the eukaryotic dsDNA African swine fever virus (ASFV) encodes a homologous DNA ligase. ASFV replicates and assembles virions in the cytoplasm of infected cells, primarily macrophages, which are highly enriched in reactive oxygen species (ROS) and subject to extensive DNA damage. The ASFV DNA ligase has been reported as a crucial component of its DNA repair system[161]. In addition to ROS, the cytosol of macrophages contains nucleases, such as TREX1[162] and DNase II[163], which degrade cytosolic DNA and prevent activation of immune pathways such as cGAS-STING (senses dsDNA in cytosol). ASFV encodes proteins that can circumvent activation of the cGAS-STING pathway, including QP383R[164]. We propose a model in which the DNA ligase functions as first line of anti-defence in ASFV, reversing effects of cytosolic nucleases and oxidative damage, while QP383R acts as a second line of anti-defence, suppressing cGAS activation despite of the presence of dsDNA in the cytosol.

Although viral DNA ligases are generally non-essential for eukaryotic virus DNA replication—as these viruses can utilise cellular DNA ligases for replication—they are essential for conferring resistance to DNA-damaging agents[165]. Normally, the cytosol of eukaryotic cells does not contain dsDNA, and several nucleases act to degrade any cytosolic DNA that arise[166–168]. Therefore, maintaining genome integrity is extremely important for DNA viruses, as DNA damage can trigger antiviral responses such as interferon (IFN)[169] or inflammasome activation[170], ultimately limiting viral propagation.

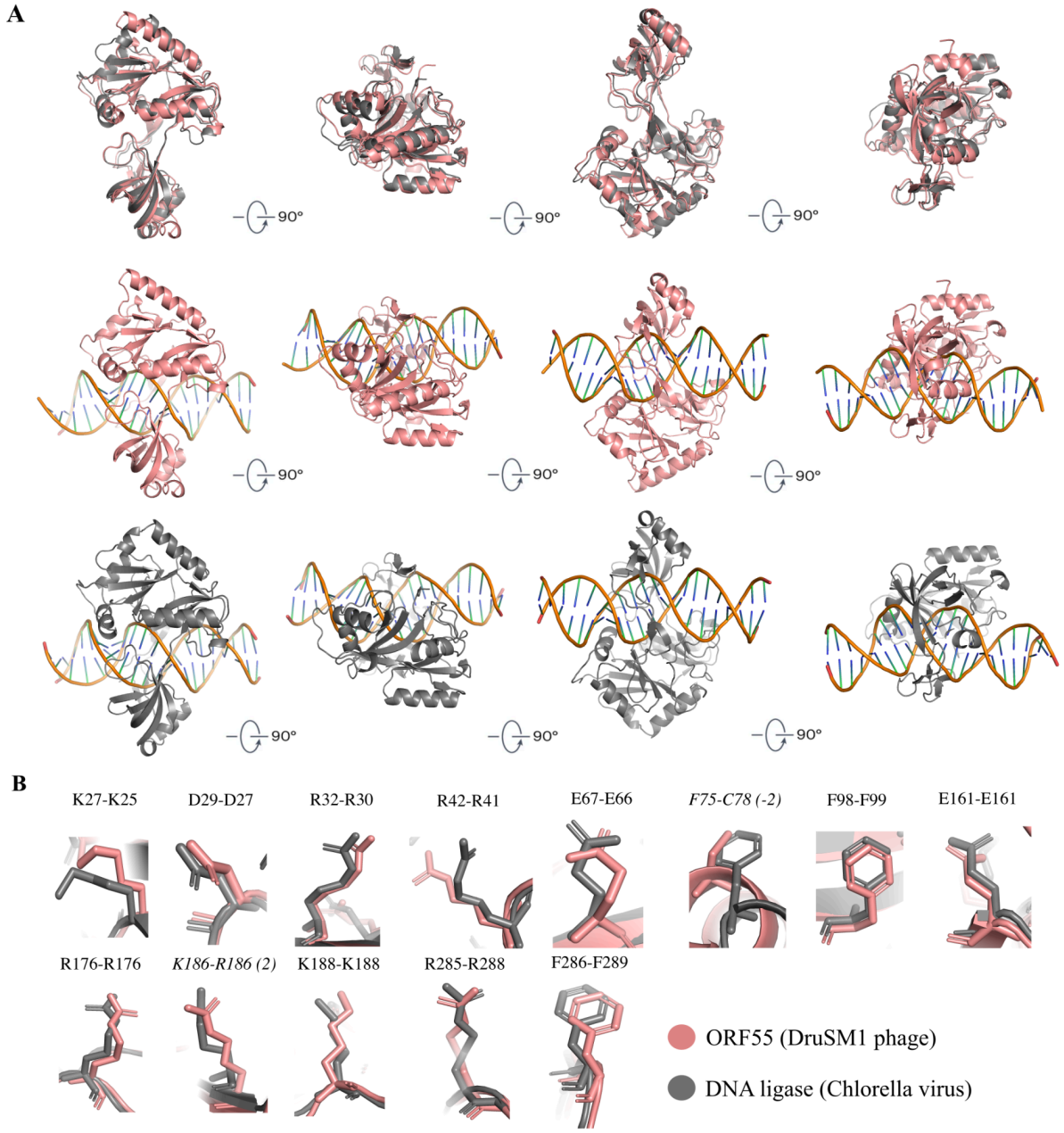

Figure 4. ORF55 shares a striking similarity with the DNA ligase from Chlorella virus.

(A) From left to right, each view represents a 90° rotation of the previous view around the x-axis. Top: superimposition of the chlorella virus DNA ligase (salmon, ribbon representation, PDB: 2Q2U) and ORF55 (grey, ribbon representation) generated using FATCAT 2.0 (p-value 0.00e+00). Middle: the DNA ligase from Chlorella virus in complex with DNA (PDB: 2Q2U). Button: a high-confidence complex between ORF55 and the DNA fragment from the complex with the DNA ligase from Chlorella virus.

(B) Thirteen residues contributing to the active site of DNA ligase (grey) are rendered as sticks aligned with the closest residues (rendered in the same way) from ORF55 (salmon).

Anti-Avs protein ORF83 is likely to bind AMP and is encoded by viruses infecting multiple amoeba species

ORF83 is an anti-type III Avs protein, originally annotated as "Smf; Predicted Rossmann fold nucleotide-binding protein DprA/Smf involved in DNA uptake"[14]. We predicted a high-quality structural model of ORF83 using AlphaFold 3 (pLDDT 95, pTM = 0.92) and searched for structural homologs in PDB[171], as before. The top-scoring matches were Cg1261 (PDB ID: 5WQ3, E-value = $4.39e^{-7}$)—a type II cytokine-activating protein from the Lonely Guy (LOG) family—along with TT1465, a hypothetical lysine decarboxylases (PDB ID: 1WEK, E-value = $7.95e^{-7}$), and DprA (PDB ID: 3UQZ, E-value = $3.49e^{-5}$).

Although TT1465 was initially predicted to be a lysine decarboxylase, experimental studies revealed that it lacks decarboxylase activity and instead exhibits phosphoribohydrolase activity[172]. Both Cg1261 and TT1465 were shown to hydrolyze AMP into adenine and ribose 5-phosphate[172]. However, among these, only Cg1261 has been experimentally confirmed to possess cytokine-activating activity and the ability the ability to convert N6-(isopentenyl)-adenosine 5′-monophosphate (iPRMP) into isopentenyladenine via dephosphoribosylation.

To investigate whether ORF83 might have similar phosphoribohydrolase activity, we modelled its interaction with AMP using AlphaFold 3, which produced a high-confidence complex (ipTM = 0.9; Figure 5). Notably, the AMP-binding region of ORF83 aligns with the corresponding AMP-interacting region of Cg1261 (Figure 5A). Structural alignment between the active site of Cg1261 and ORF83 revealed that they share two invariant residues (R115/R89 and T175/T112), along with one conservative substitution (E178/D114) and a neutral substitution (K116/N90). Given the high structural similarity between ORF83 and Cg1261, the confidently predicted AMP interaction, and the partial conservation of active site residues, we propose that ORF83 likely possesses phosphoribohydrolase activity towards AMP. However, the residue composition of ORF83 diverges from that of Cg1261 at the prenyl-binding site, thus providing no structural evidence that ORF83 binds iPRMP or functions as a cytokine-activating protein.

We also examined the lower-scoring structural similarity between ORF83 and DprA, a protein involved in DNA transformation that forms a complex with RecA[173]. DprA is a protein involved in DNA transformation and acts in a complex with the RecA protein[173]. DprA's function relies on residues critical for self-dimerisation and RecA binding. Structural alignment revealed that these key residues are poorly conserved in ORF83, both in sequence and in spatial configuration, suggesting that ORF83 is unlikely to perform DprA-like functions. Moreover, AlphaFold 3 predicted a complex between ORF83 and RecA with an ipTM score of 0.18, indicating that the interaction is unlikely. In conclusion, our data support the prediction that ORF83 interacts with AMP and likely exhibits phosphoribohydrolase activity. However, experimental validation is required to confirm this function and to determine how it contributes to evasion of the type III Avs defence system.

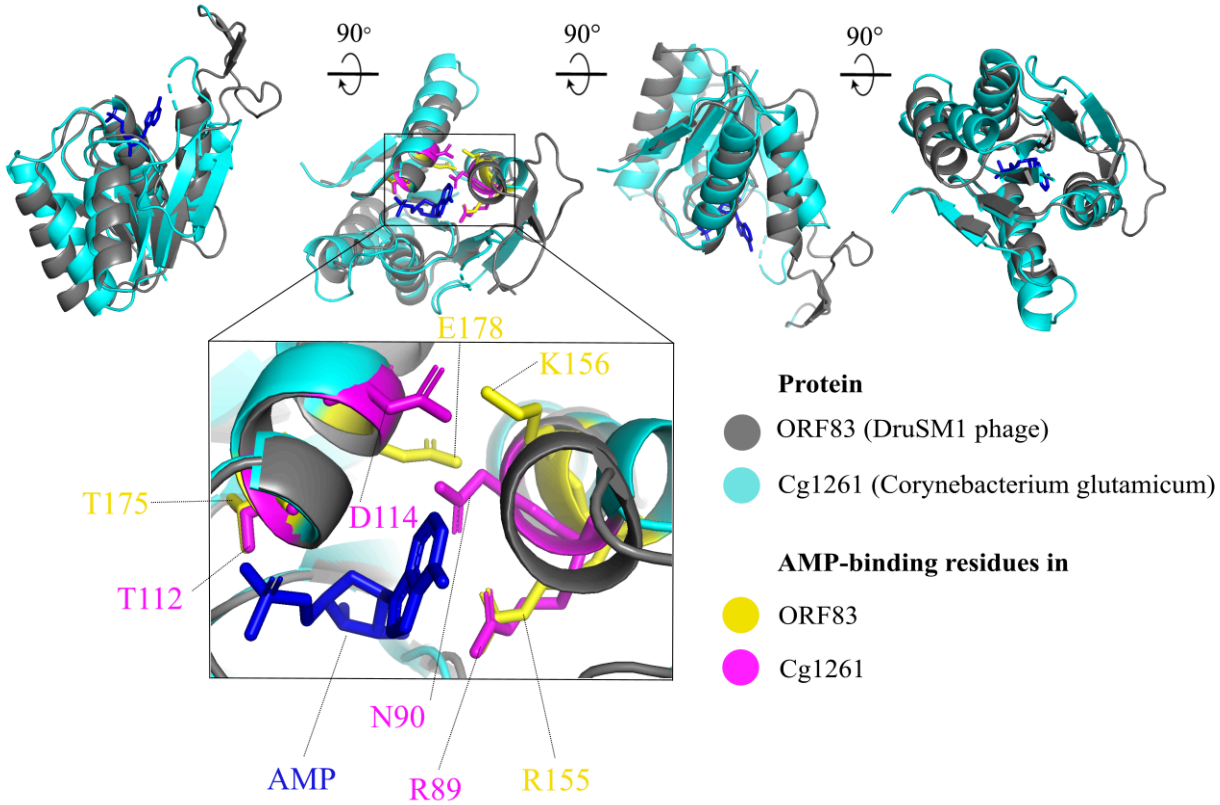

Figure 5. ORF83 is homologous to cytokine activating protein Cg1291 and binds AMP.

Four different views of the superimposition of the AMP (blue, stick representation)-ORF83 (grey, ribbon representation) complex (AlphaFold 3 prediction) with the type II cytokine-activating protein Cg1261 (cyan, ribbon representations) of the LOG family, generated using FATCAT 2.0 (p-value = 4.39e-7), each related by a 90º rotation around the x-axis. The second view provides the best orientation of the AMP-binding site, which is expanded in the bottom insert. Residues in Cg1261, characterized as part of the AMP-binding active site, are colored magenta, and the closest residues in ORF83 are colored yellow (corresponding to AMP-binding residues predicted by AlphaFold 3).

We found 14 homologs of ORF83 in eukaryotic viruses that infect various amoeba species. Interestingly, many homologs are longer and contain the domain DUF4326 at the C-terminus. For instance, YP_009506880 from *Tunisvirus fontaine 2* shares extremely high structural similarity to ORF83 (p-value = 2.99^{e-13}; Figure 6). We predicted its complex with AMP using AlphaFold 3 (ipTM = 0.85, pTM = 0.77). The alignment between ORF83 and YP_009506880 showed that they share the same putative AMP-binding active site (R89-R73, N90-N74, and T112-T95 in ORF83 and YP_009506880, respectively), differing only by one neutral substitution (D114-S97). Overall, these results demonstrate functional homology between ORF83, the anti-Avs protein from phages—and YP_009506880, the protein from eukaryotic viruses.

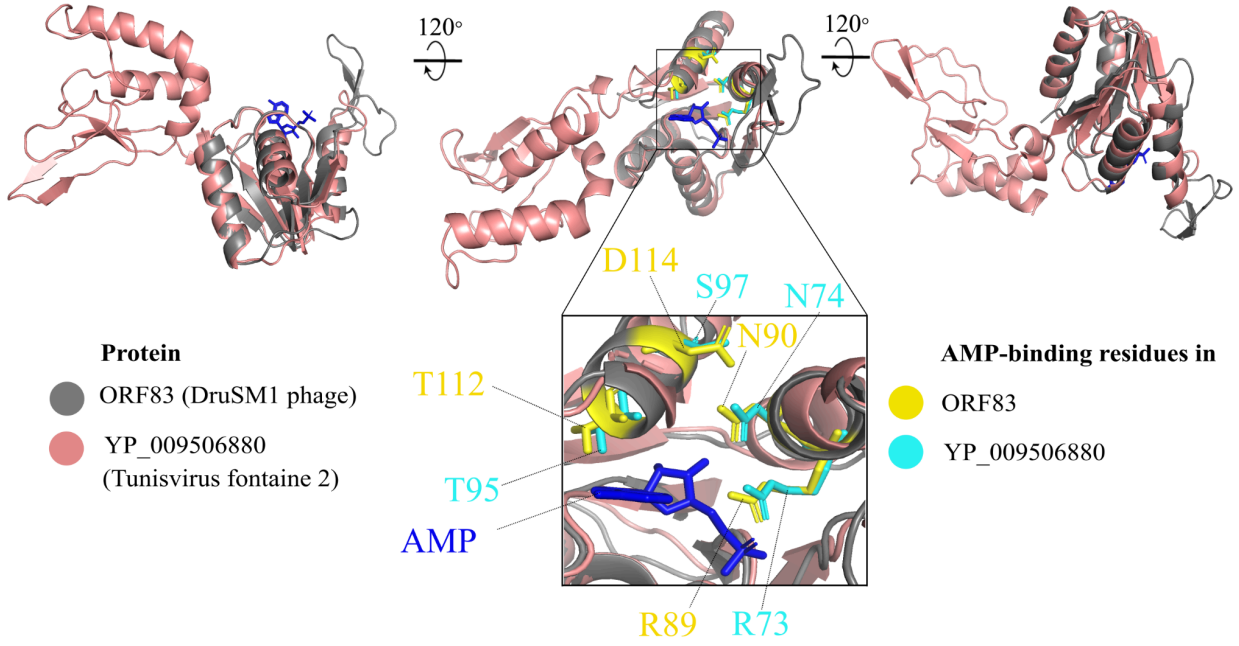

Figure 6. ORF83 has homologs in dsDNA viruses.

Three different views of the superimposition of the complex between AMP (blue, stick representation) and a protein from *Tunisvirus fontaine 2* (salmon, ribbon representation, NCBI GenPept accession: YP_009506880) with the phage protein ORF83 (grey, ribbon representation), generated using FATCAT 2.0 (p-value = 2.99e-13) each related by a 120° rotation around the x-axis. The second view provides the best orientation of the AMP-binding site, which is expanded in the bottom insert. AMP-binding active site residues of ORF83 are shown in yellow, and those of YP_009506880's are shown in cyan.

Phage nucleotidyltransferase homologs in eukaryotic viruses

The cyclic GMP–AMP synthase (cGAS)-STING pathway is a conserved immune mechanism found in both bacteria and eukaryotes. It is characterised by sensory cGAS proteins that synthesise cyclic nucleotides in response to viral infections. These nucleotides bind the STING domain-containing effector proteins, which initiate downstream immune responses. In bacteria, these effectors typically cleave NAD+, whereas in eukaryotes they activate the expression of antiviral genes.

A nucleotidyltransferase (NTase) enzyme from *Bacillus* phage Bcp1 (NCBI GenPept accession: YP_009031408) synthesises a competing cyclic nucleotide, 3′,3′-cyclic GMP-AMP (3′,3′-cGAMP), which inhibits the cGAS-STING response[50]. We identified 12 homologs of this phage NTase in a range of eukaryotic viruses that infect insects, suggesting a potential role in suppressing the eukaryotic cGAS-STING pathway. For instance, YP_009091875 from *Erinnyis ello* granulovirus—which infects *Erinnyis* species—shows high structural similarity to the phage NTase (Figure 7A; FATCAT 2.0 p-value 3.10e-10). Importantly, Ho *et al.* identified two catalytic

motifs for phage NTases: **GS-x-AY[GAN]T-x4-SDxD** and **NP-x-h2[DE]**. The second motif (**NP-x-h2[DE])** appears to be unique to phage NTases within the broader NTase superfamily. Notably, the *Erinnyis ello* granulovirus protein exhibits comparable similarity to the consensus active site motifs as the Bcp1 NTase (Figure 7B), matching 10 out of 14 conserved positions, whereas the phage NTase with experimentally verified inhibitory activity against cGAS-STING response matches 11 out of 14 positions.

Nucleoside triphosphates (NTPs) serve as ligands in cyclic nucleotide synthesis, with metal ions such as Mg2+ typically acting as catalytic cofactors [174]. To investigate functional mechanisms of these NTases further, we modeled interactions between NTPs used in cyclic nucleotide synthesis (ATP, GTP and UTP) with both the phage NTase and its homolog in *Erinnyis ello* granulovirus using AlphaFold 3.

All predicted complexes yielded ipTM scores above 0.8 (Figure 7C), indicating high-confidence predictions, and the predicted ipTM scores for complexes of phage and viral proteins show strong correlation (Pearson correlation = 0.865, p-value 0.0261), likely indicating similar substrate preferences. The highest-scoring complex produced for both proteins includes two molecules of UTP and three ions of Mg^{2+}. We show that the highest-confidence complex predicted for protein from *Erinnyis ello* granulovirus granulovirus uses a similar configuration of the active site as EcCdnD, in which two Mg^{2+} ions coordinate the donor NTP and one Mg^{2+} ion coordinates the acceptor NTP (Figure 7D)[174]. Moreover, we visualised the residues forming bounds with NTPs and ions and showed that conserved motif **SDxD** is particularly important, similar to the E-clade of CD-NTases[174] (Figure 7D).

Given the high structural similarity between the phage NTase and putative NTases from the dsDNA eukaryotic viruses, their conserved active site residues, and high-confidence predictions of protein-NTP/NDP-Mg2+ complex formation, we postulate that the viral protein synthesize cyclic nucleotides. This activity may enable eukaryotic dsDNA viruses to evade the cGAS-STING response—a ubiquitous innate immune pathway that senses dsDNA in cytosol of eukaryotic cells.

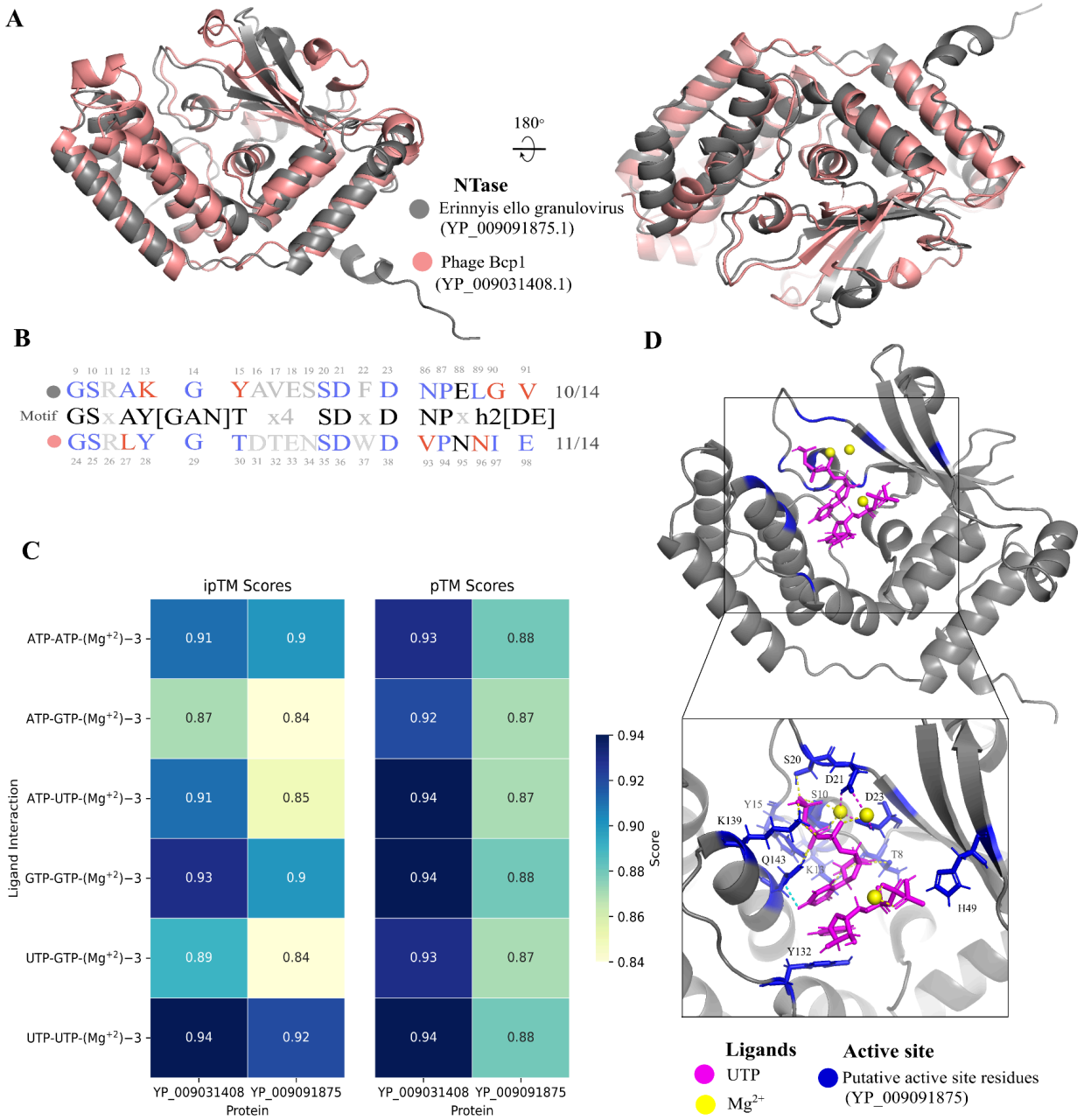

Figure 7. Structural and Functional Analysis of NTase from Bacillus Phage Bcp1 and Erinnyis ello Granulovirus

(A) Left, structural alignment of the cyclic nucleotide-synthesizing NTase from *Bacillus* phage Bcp1 (salmon, NCBI GenPept accession: YP_009031408) and its homolog from *Erinnyis ello* granulovirus (grey, NCBI GenPept accession: YP_009091875), performed using FATCAT 2.0 (p-value: 2.74e-10). Right, the view of the structural alignment is rotation 180° around the X-axis.

(B) Alignment of catalytic site motifs of phage NTases (middle row) to the experimentally validated NTase from *Bacillus* phage Bcp1 (bottom row) and its homolog from the dsDNA eukaryotic virus (YP_009091875 from *Erinnyis ello* granulovirus, top row). Matches are in blue, mismatches in red, and residues matching variable motif positions in the sequence motif are in grey.

(C) Heatmap of confidence scores (ipTM and pTM, where light blue indicates lo) for complexes between phage or viral NTases with pairs of NTPs and three ions of Mg^{2+} produced by AlphaFold 3.

(D) Predicted complex of *Erinnyis ello* granulovirus NTase (grey) with two molecules of UTP (magenta) and three ions of Mg2+ (yellow), the active site residues in the NTase are in blue.

DISCUSSION

We have curated a comprehensive database of phage ADPs, called EVADES. This database encompasses a greater diversity of ADPs than other resources, such as Anti-DefenseFinder or dbAPIS. Over and above the number of ADPs, its principal distinction lies in providing insights into MoA, as well as cataloguing both experimental and predicted structures, information about protein family membership, and the potential to trigger bacterial defence systems. We also categorised phage ADPs based on their MoA. While most ADPs remain uncharacterised, the most prevalent functional characterised category is direct binders – phage proteins that directly interact with bacterial defence proteins to inhibit their activity. We believe this functional information can facilitate biological insights. For instance, knowing that the majority of ADPs are direct binders, we hypothesised that some uncharacterised ADPs may inhibit bacterial defences through binding. To test this hypothesis, we modelled the interactions between uncharacterised ADPs and the defence systems they inhibit using AlphaFold 3, and predicted interactions for 20 ADPs. Where possible, we cross-referenced the predicted complexes and experimental data and found that our predictions align with the experimental results. One exciting example is AcrIB4, a protein that was reported as a Cas8b homolog (sharing 38% identity with the last 90 residues); however, it was not replacing Cas8b in the Cascade complex, as is usually expected with ADPs sharing similarity to subunits of defence systems. We predicted that AcrIB4 binds to Cas8b, specifically interacting with the residues in Cas8b that bind to the Cas11 protein, which stabilises the Cascade complex. Cas11 is translated from an internal ribosome-binding site within the 3′ end of the *cas8b* gene, suggesting that AcrIB4 is homologous to Cas11. We propose that AcrIB4 acts as a Cas11 replacement, destabilising the Cascade complex. To the best of our knowledge, this is the first example of an Acr acting through complex subunit poisoning by replacing Cas11.

We found that many ADPs, while inhibiting one defence system, actually trigger another. Typically, these ADPs are widespread and inhibit ubiquitous defence systems that cleave phage genetic material, while triggering defences that induce abortive infection. We speculate that this could be a common phenomenon in phage–host interactions, as bacteria evolve counter-counter-defence systems in response to phage anti-defence strategies. Furthermore, we hypothesise that bacterial defence systems operate in layers, where systems that cleave foreign nucleic acids and cause minimal collateral damage serve as the first line of defence. In contrast, systems that trigger abortive infection may sense the inhibition of these first-line

defences, providing maximum protection while minimising self-damage. Such interactions between defence systems may also explain the distribution of these systems in bacterial populations, where certain pairs are frequently encoded together due to their evolutionary advantages. We showed that ADPs that trigger bacterial defence systems are enriched in those ADPs that act as DNA mimics. We predicted broad-spectrum direct interactions between DNA mimics and bacterial defence proteins, unsurprisingly, particularly those that bind DNA. This layering of defence systems could be explained by the evolutionary pressure exerted by DNA mimics on bacteria, as they can inhibit numerous DNA-binding defence systems, thereby driving the evolution of bacterial counter-counter adaptations.

We provide evidence that homologs of phage ADPs can be found in eukaryotic dsDNA viruses, where they evade eukaryotic immunity. It has been widely proposed that eukaryotic dsDNA viruses evolved from phages, and that eukaryotic immune systems have evolved from bacterial defence systems. We identified numerous homologues of phage anti-defence systems in eukaryotic viruses, including those infecting humans. Among these, we focused on proteins that evade defence systems shared between prokaryotes and eukaryotes, such as the cGAS–STING response and the Avs systems, which are homologous to the STAND superfamily utilised in eukaryotic innate immunity. For instance, we found that dsDNA viruses encode structural and functional homologues of phage NTases, which inhibit the bacterial cGAS–STING response by producing competing cyclic nucleotides. In eukaryotes, cGAS–STING functions as a cytosolic dsDNA-sensing innate immune pathway.

We also proposed a mechanism of action for the anti-Avs protein ORF55, demonstrating its involvement in DNA repair to counteract the effects of Avs effector nucleases. This conclusion was supported by its similarity to a minimal DNA ligase from the eukaryotic dsDNA Chlorella virus.

These findings have far-reaching implications for understanding how eukaryotic viruses evade the host immune system, with mechanisms being informed by insights gained from studying phages. The extensive body of research in this field underscores the potential for reciprocal learning between phage and eukaryotic viral systems.

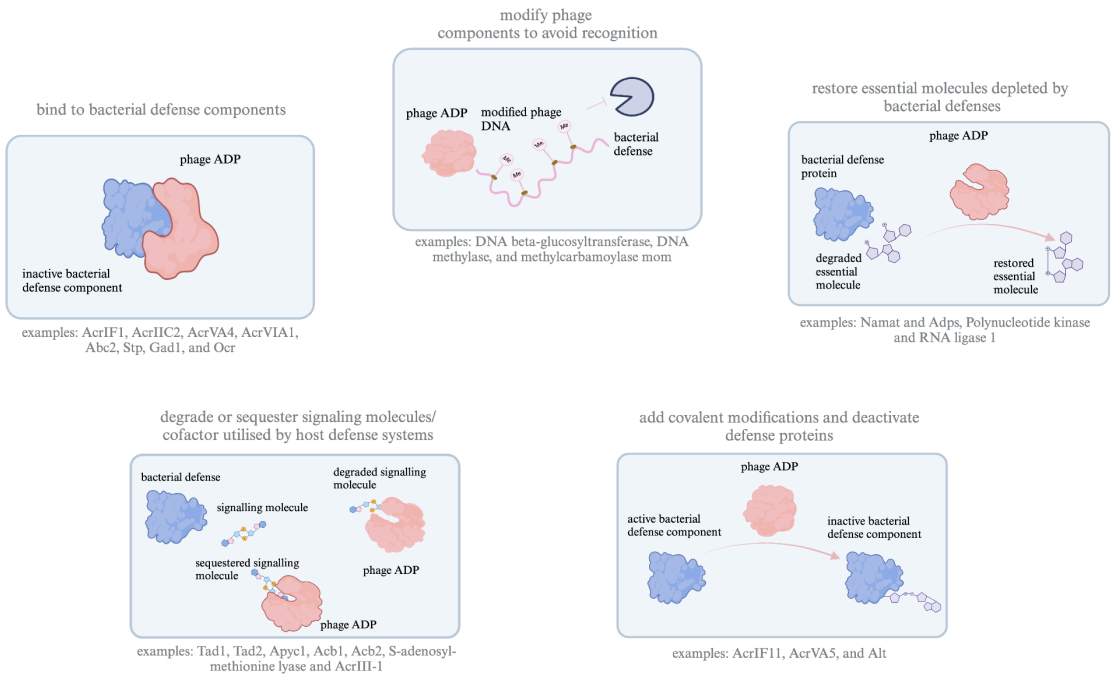

Supplementary Figure 1. Classification of phage ADPs based on mechanism of action. ADPs

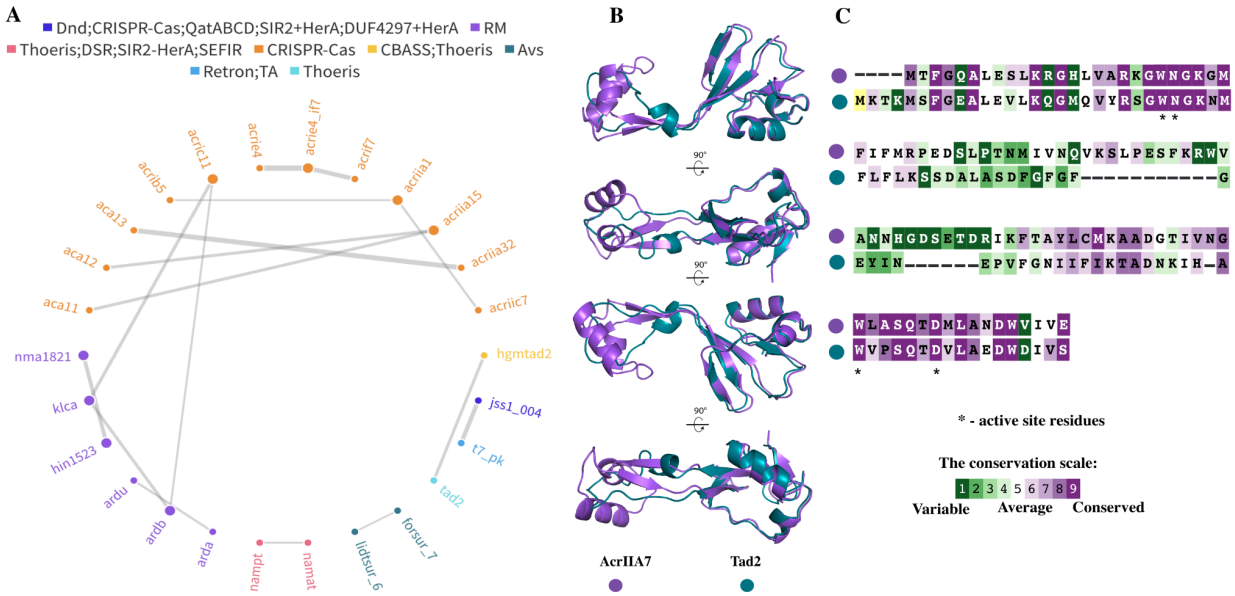

Supplementary figure 2. Similarity between AcrIIA7 and Tad2

(A) ADP sequence similarity network -ADP node size is proportional to number of proteins an ADP shares similarity to and nodes are colored based on the defence system(s) they inhibit, edge width is proportional to shared sequence identity.

(B) Structural alignment between AcrIIA7's structural model (purple) produced by AlphaFold 3 and Tad2 (teal blue, PDB ID: 8SMG) obtained with FATCAT 2.0 (p-value: 2.55e-8). From top to bottom, each view represents a 90° rotation of the previous view around the Y-axis.

(C) Sequence alignment between AcrIIA7 and Tad (based on structural alignment produced by FATCAT 2.0), residues are coloured based on conservation scores produced by Consurf. Active site residues denoted by asterisk (*).

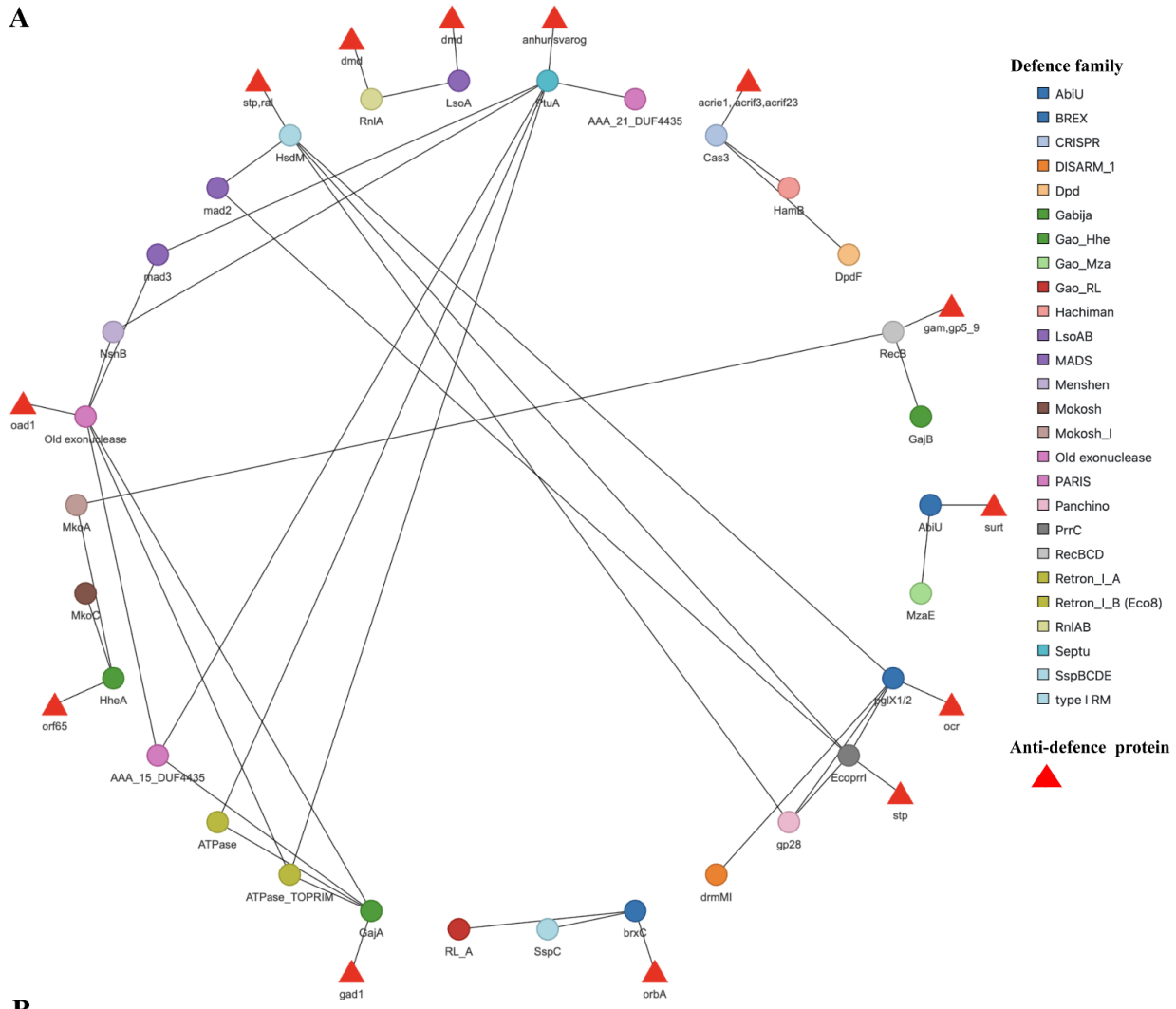
A
dmd
anhur,svarog
dmd
stp,rat
RnlA
LsoA
PtuA
AAA_21_DUF4435
acrie1,acrif3,acrif23
HsdM
Cas3
mad2
HamB
mad3
DpdF
NshB
gam,gp5_9
RecB
oad1
Old exonuclease
GajB
MkoA
AbiU
surt
MkoC
MzaE
HheA
pglX1/2
orf65
ocr
AAA_15_DUF4435
EcoprrI
stp
ATPase
gp28
ATPase_TOPRIM
drmMI
GajA
RL_A
SspC
brxC
gad1
orbA
Defence family
AbiU
BREX
CRISPR
DISARM_1
Dpd
Gabija
Gao_Hhe
Gao_Mza
Gao_RL
Hachiman
LsoAB
MADS
Menshen
Mokosh
Mokosh_I
Old exonuclease
PARIS
Panchino
PrrC
RecBCD
Retron_I_A
Retron_I_B (Eco8)
RnlAB
Septu
SspBCDE
type I RM
Anti-defence protein

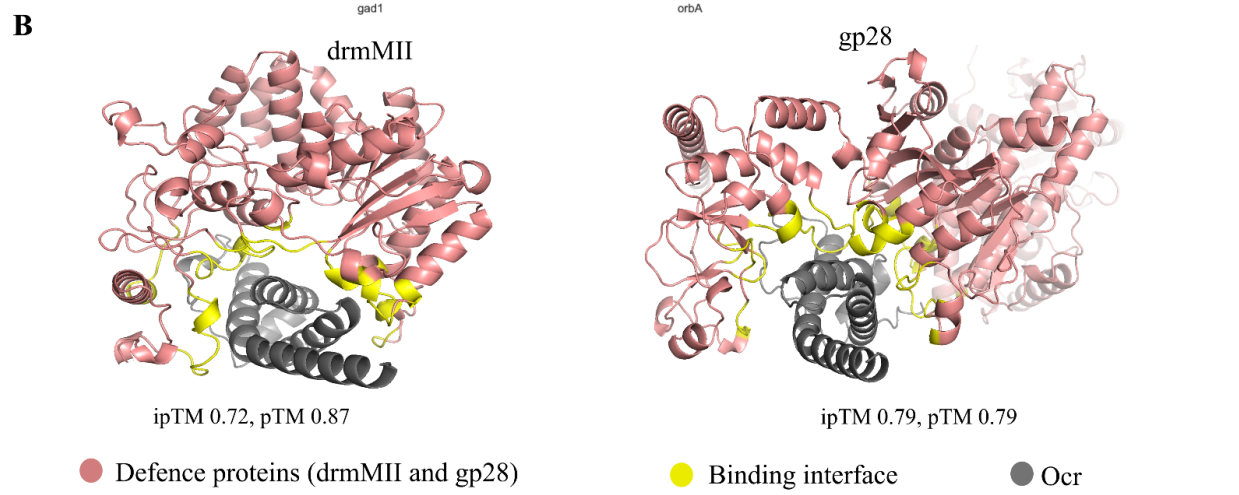
B
drmMII
gp28
ipTM 0.72, pTM 0.87
ipTM 0.79, pTM 0.79
Defence proteins (drmMII and gp28)
Binding interface
Ocr

Supplementary figure 3. Defence protein sharing can mediate multi-defence inhibitory activity of ADPs.

(A) Defence protein (circle nodes, coloured according to the defence system family) similarity network, where edges denote protein pairs that have similar structural folds (FoldSeek e-value < 1.0e-8). ADPs inhibiting the defence system directly or inhibiting single-protein defence systems are denoted as triangular nodes and are connected to the defence protein they target by an edge. **(B)** Complexes Ocr(grey)-drmMII(salmon) and Ocr(grey)-gp28(salmon) predicted by AlphaFold 3. Binding interfaces in drmMII/gp28 are shown in yellow.

Limitations of the study

Our resource paper provides a comprehensive collection of phage ADPs and proposes several hypotheses which are based on in-depth computational analysis, but are yet to be supported by experimental validation. To enable the users of EVADES to understand those functions that are predicted versus experimentally validated, MoA are labelled with evidence code ontologies. In this paper and the resource, we have focused on confident predictions, reducing the chances of false positives.

Lead contact

Further information and requests for resources should be directed to and will be fulfilled by the lead contact, Robert D. Finn (rdf@ebi.ac.uk).

Data and code availability

- The database is publicly available at: https://www.ebi.ac.uk/finn-srv/evades

ACKNOWLEDGMENTS

K.M., F.C, and R.D.F. are funded by the European Molecular Biology Laboratory (EMBL). E.K. is an ARISE Fellow and received funding from the European Union's Horizon 2020 research and innovation programme under the Marie Skłodowska-Curie grant agreement No 945405. J.W. was a recipient of Marie Skłodowska-Curie Postdoctoral Fellowship, EMBL Interdisciplinary Postdoctoral (EIPOD) Fellowship and EMBO Non-Stipendiary Fellowship (EMBO ALTF 400-2022), and a Junior Research Fellow at Wolfson College, the University of Cambridge, UK.

We would like to thank the MGnify service team members – Mahfouz Shehu, Aleksandar Rajkovic, Martin Beracochea and Sandy Rogers, for their technical assistance and code review, and Anna Lopatina for insightful discussions.

AUTHOR CONTRIBUTIONS

Conceptualization, K.M. and R.D.F.; methodology, K.M., E.K. and R.D.F.; Investigation, K.M., J.W., F.C.; writing—original draft, K.M.; writing—review & editing, K.M., F.C., E.K., J.W. and R.D.F.; funding acquisition, R.D.F.; resources, E.K. and K.M.; supervision, K.M. and R.D.F.

DECLARATION OF INTERESTS

The authors declare no competing interests.

DECLARATION OF GENERATIVE AI AND AI-ASSISTED TECHNOLOGIES

During the preparation of this work, the authors used ChatGPT in order to improve grammar. After using this tool or service, the authors reviewed and edited the content as needed and take full responsibility for the content of the publication.

SUPPLEMENTAL INFORMATION

Document S1. Figures S1–S3 and Table S1-S7
Table S1. Comparison of EVADES with dbAPIS and Anti-Defense Finder in terms of sequence diversity and defence families
Table S2. Structural similarity between defence proteins
Table S3. Uncharacterised ADPs and protein from counteracted defence systems
Table S4. Moderate and high-confidence complexes predicted for uncharacterised ADPs
Table S5. DNA mimic
Table S6. High-confidence complexes predicted between DNA mimics and defence proteins
Table S7. Predicted ipTM/pTM scores for complexes between pairs of NTPs, three ions of Mg^{2+} and YP_009091875 or YP_009031408.

REFERENCES

1. Georjon, H., and Bernheim, A. (2023). The highly diverse antiphage defence systems of bacteria. Nat. Rev. Microbiol. https://doi.org/10.1038/s41579-023-00934-x.

2. Tal, N., and Sorek, R. (2022). SnapShot: Bacterial immunity. Cell *185*, 578–578.e1.

3. Murtazalieva, K., Mu, A., Petrovskaya, A., and Finn, R.D. (2024). The growing repertoire of phage anti-defence systems. Trends Microbiol. *0*. https://doi.org/10.1016/j.tim.2024.05.005.

4. Mayo-Muñoz, D., Pinilla-Redondo, R., Camara-Wilpert, S., Birkholz, N., and Fineran, P.C. (2024). Inhibitors of bacterial immune systems: discovery, mechanisms and applications. Nat. Rev. Genet. https://doi.org/10.1038/s41576-023-00676-9.

5. Nadendla, S., Jackson, R., Munro, J., Quaglia, F., Mészáros, B., Olley, D., Hobbs, E.T., Goralski, S.M., Chibucos, M., Mungall, C.J., et al. (2022). ECO: the Evidence and Conclusion Ontology, an update for 2022. Nucleic Acids Res. *50*, D1515–D1521.

6. Bartolec, T., Mitosch, K., Potel, C., Corona, F., Yang, A.L.J., Burtscher, M.L., Koumoutsi, A., Becher, I., Bobonis, J., Karcher, N., et al. (2024). Pervasive phosphorylation by phage T7 kinase disarms bacterial defenses. bioRxiv. https://doi.org/10.1101/2024.12.20.629319.

7. Jiang, S., Chen, C., Huang, W., He, Y., Du, X., Wang, Y., Ou, H., Deng, Z., Xu, C., Jiang, L., et al. (2024). A widespread phage-encoded kinase enables evasion of multiple host antiphage defence systems. Nat. Microbiol. *9*, 3226–3239.

8. Li, D., Xiao, Y., Fedorova, I., Xiong, W., Wang, Y., Liu, X., Huiting, E., Ren, J., Gao, Z., Zhao, X., et al. (2024). Single phage proteins sequester signals from TIR and cGAS-like enzymes. Nature *635*, 719–727.

9. Yirmiya, E., Leavitt, A., Lu, A., Ragucci, A.E., Avraham, C., Osterman, I., Garb, J., Antine, S.P., Mooney, S.E., Hobbs, S.J., et al. (2023). Phages overcome bacterial immunity via diverse anti-defence proteins. Nature. https://doi.org/10.1038/s41586-023-06869-w.

10. Leavitt, A., Yirmiya, E., Amitai, G., Lu, A., Garb, J., Herbst, E., Morehouse, B.R., Hobbs, S.J., Antine, S.P., Sun, Z.-Y.J., et al. (2022). Viruses inhibit TIR gcADPR signalling to overcome bacterial defence. Nature *611*, 326–331.

11. Drobiazko, A., Adams, M.C., Skutel, M., Potekhina, K., Kotovskaya, O., Trofimova, A., Matlashov, M., Yatselenko, D., Maxwell, K.L., Blower, T.R., et al. (2025). Molecular basis of foreign DNA recognition by BREX anti-phage immunity system. Nat. Commun. *16*, 1825.

12. Andriianov, A., Trigüis, S., Drobiazko, A., Sierro, N., Ivanov, N.V., Selmer, M., Severinov, K., and Isaev, A. (2023). Phage T3 overcomes the BREX defense through SAM cleavage and inhibition of SAM synthesis by SAM lyase. Cell Rep. *42*, 112972.

13. Osterman, I., Samra, H., Rousset, F., Loseva, E., Itkin, M., Malitsky, S., Yirmiya, E., Millman, A., and Sorek, R. (2024). Phages reconstitute NAD+ to counter bacterial immunity. Nature *634*, 1160–1167.

14. Ojima, S., Azam, A.H., Kondo, K., Nie, W., Wang, S., Chihara, K., Tamura, A., Yamashita, W., Nakamura, T., Sugawara, Y., et al. (2024). Systematic discovery of phage genes that inactivate bacterial immune systems. bioRxiv, 2024.04.14.589459. https://doi.org/10.1101/2024.04.14.589459.

15. Lopatina, A., Ferenc, M., Bartlau, N., Wolfram, M., Steensen, K., Muscia, S., Hussain, F., Schnurer, M., Afjehi-Sadat, L., Pollak, S., et al. (2024). Interpretable machine learning reveals a diverse arsenal of anti-defenses in bacterial viruses. bioRxiv, 2024.06.14.598830. https://doi.org/10.1101/2024.06.14.598830.

16. Bernheim, A., Cury, J., and Poirier, E.Z. (2024). The immune modules conserved across the tree of life: Towards a definition of ancestral immunity. PLoS Biol. *22*, e3002717.

17. Millman, A., Bernheim, A., Stokar-Avihail, A., Fedorenko, T., Voichek, M., Leavitt, A., Oppenheimer-Shaanan, Y., and Sorek, R. (2020). Bacterial Retrons Function In Anti-Phage Defense. Cell *183*, 1551–1561.e12.

18. Penner, M., Morad, I., Snyder, L., and Kaufmann, G. (1995). Phage T4-coded Stp: double-edged effector of coupled DNA and tRNA-restriction systems. J. Mol. Biol. *249*, 857–868.

19. Rousset, F., Depardieu, F., Miele, S., Dowding, J., Laval, A.-L., Lieberman, E., Garry, D., Rocha, E.P.C., Bernheim, A., and Bikard, D. (2022). Phages and their satellites encode hotspots of antiviral systems. Cell Host Microbe *30*, 740–753.e5.

20. Bobonis, J., Mitosch, K., Mateus, A., Karcher, N., Kritikos, G., Selkrig, J., Zietek, M., Monzon, V., Pfalz, B., Garcia-Santamarina, S., et al. (2022). Bacterial retrons encode phage-defending tripartite toxin-antitoxin systems. Nature *609*, 144–150.

21. Wein, T., Millman, A., Lange, K., Yirmiya, E., Hadary, R., Garb, J., Melamed, S., Amitai, G., Dym, O., Steinruecke, F., et al. (2025). CARD domains mediate anti-phage defence in bacterial gasdermin systems. Nature, 1–8.

22. Deep, A., Liang, Q., Enustun, E., Pogliano, J., and Corbett, K.D. (2024). Architecture and activation mechanism of the bacterial PARIS defence system. Nature *634*, 432–439.

23. Amitsur, M., Benjamin, S., Rosner, R., Chapman-Shimshoni, D., Meidler, R., Blanga, S., and Kaufmann, G. (2003). Bacteriophage T4-encoded Stp can be replaced as activator of anticodon nuclease by a normal host cell metabolite: Alternative modes of anticodon nuclease activation. Mol. Microbiol. *50*, 129–143.

24. Silas, S., Carion, H., Makarova, K.S., Laderman, E.S., Todeschini, T., Kumar, P., Johnson, M., Bocek, M., Nobrega, F.L., Koonin, E.V., et al. (2025). Activation of bacterial programmed cell death by phage inhibitors of host immunity. Mol. Cell *85*, 1838–1851.e10.

25. Stokar-Avihail, A., Fedorenko, T., Hör, J., Garb, J., Leavitt, A., Millman, A., Shulman, G., Wojtania, N., Melamed, S., Amitai, G., et al. (2023). Discovery of phage determinants that confer sensitivity to bacterial immune systems. Cell *186*, 1863–1876.e16.

26. Liu, C., Wang, R., Li, Z., Wang, W., Yao, J., Cheng, F., Du, X., Guan, L., Mestre, M.R., Xu, J., et al. (2024). Phage CRISPR-like regulatory RNAs silence bacterial adaptive and innate immunity. bioRxiv, 2024.10.29.618823. https://doi.org/10.1101/2024.10.29.618823.

27. Wein, T., Johnson, A.G., Millman, A., Lange, K., Yirmiya, E., Hadary, R., Garb, J., Steinruecke, F., Hill, A.B., Kranzusch, P.J., et al. (2023). CARD-like domains mediate anti-phage defense in bacterial gasdermin systems. bioRxiv, 2023.05.28.542683. https://doi.org/10.1101/2023.05.28.542683.

28. Ledvina, H.E., and Whiteley, A.T. (2024). Conservation and similarity of bacterial and eukaryotic innate immunity. Nat. Rev. Microbiol. *22*, 420–434.

29. Wein, T., and Sorek, R. (2022). Bacterial origins of human cell-autonomous innate immune mechanisms. Nat. Rev. Immunol. *22*, 629–638.

30. Koonin, E.V., Krupovic, M., and Yutin, N. (2015). Evolution of double-stranded DNA viruses of eukaryotes: from bacteriophages to transposons to giant viruses: Evolution of dsDNA viruses of eukaryotes. Ann. N. Y. Acad. Sci. *1341*, 10–24.

31. Koonin, E.V., and Yutin, N. (2010). Origin and evolution of eukaryotic large nucleo-cytoplasmic DNA viruses. Intervirology *53*, 284–292.

32. Iranzo, J., Krupovic, M., and Koonin, E.V. (2016). The double-stranded DNA virosphere as a modular hierarchical network of gene sharing. MBio *7*. https://doi.org/10.1128/mBio.00978-16.

33. Hobbs, S.J., Nomburg, J., Doudna, J.A., and Kranzusch, P.J. (2024). Animal and bacterial viruses share conserved mechanisms of immune evasion. Cell *187*, 5530–5539.e8.

34. Yirmiya, E., Hobbs, S.J., Leavitt, A., Osterman, I., Avraham, C., Hochhauser, D., Madhala, B., Skovorodka, M., Tan, J.M.J., Toyoda, H.C., et al. (2025). Structure-guided discovery of viral proteins that inhibit host immunity. Cell *0*. https://doi.org/10.1016/j.cell.2024.12.035.

35. Bondy-Denomy, J., Pawluk, A., Maxwell, K.L., and Davidson, A.R. (2013). Bacteriophage genes that inactivate the CRISPR/Cas bacterial immune system. Nature *493*, 429–432.

36. León, L.M., Park, A.E., Borges, A.L., Zhang, J.Y., and Bondy-Denomy, J. (2021). Mobile element warfare via CRISPR and anti-CRISPR in Pseudomonas aeruginosa. Nucleic Acids Res. *49*, 2114–2125.

37. Song, G., Zhang, F., Tian, C., Gao, X., Zhu, X., Fan, D., and Tian, Y. (2022). Discovery of potent and versatile CRISPR-Cas9 inhibitors engineered for chemically controllable genome editing. Nucleic Acids Res. *50*, 2836–2853.

38. Pawluk, A., Staals, R.H.J., Taylor, C., Watson, B.N.J., Saha, S., Fineran, P.C., Maxwell, K.L., and Davidson, A.R. (2016). Inactivation of CRISPR-Cas systems by anti-CRISPR proteins in diverse bacterial species. Nat. Microbiol. *1*, 16085.

39. Pawluk, A., Amrani, N., Zhang, Y., Garcia, B., Hidalgo-Reyes, Y., Lee, J., Edraki, A., Shah, M., Sontheimer, E.J., Maxwell, K.L., et al. (2016). Naturally occurring off-switches for CRISPR-Cas9. Cell *167*, 1829–1838.e9.

40. Marino, N.D., Zhang, J.Y., Borges, A.L., Sousa, A.A., Leon, L.M., Rauch, B.J., Walton, R.T., Berry, J.D., Joung, J.K., Kleinstiver, B.P., et al. (2018). Discovery of widespread type I and type V CRISPR-Cas inhibitors. Science *362*, 240–242.

41. He, F., Bhoobalan-Chitty, Y., Van, L.B., Kjeldsen, A.L., Dedola, M., Makarova, K.S., Koonin, E.V., Brodersen, D.E., and Peng, X. (2018). Anti-CRISPR proteins encoded by archaeal lytic viruses inhibit subtype I-D immunity. Nat. Microbiol. *3*, 461–469.

42. Pinilla-Redondo, R., Shehreen, S., Marino, N.D., Fagerlund, R.D., Brown, C.M., Sørensen, S.J., Fineran, P.C., and Bondy-Denomy, J. (2020). Discovery of multiple anti-CRISPRs highlights anti-defense gene clustering in mobile genetic elements. Nat. Commun. *11*, 5652.

43. Gao, L.A., Wilkinson, M.E., Strecker, J., Makarova, K.S., Macrae, R.K., Koonin, E.V., and Zhang, F. (2022). Prokaryotic innate immunity through pattern recognition of conserved viral proteins. Science *377*, eabm4096.

44. LeGault, K.N., Hays, S.G., Angermeyer, A., McKitterick, A.C., Johura, F.-T., Sultana, M., Ahmed, T., Alam, M., and Seed, K.D. (2021). Temporal shifts in antibiotic resistance elements govern phage-pathogen conflicts. Science *373*. https://doi.org/10.1126/science.abg2166.

45. Silas, S., Carion, H., Makarova, K.S., Laderman, E., Godinez, D.S., Johnson, M., Fossati, A., Swaney, D., Bocek, M., Koonin, E.V., et al. (2023). Parallelized screening of virus accessory genes reveals diverse defense and counter-defense mechanisms. bioRxiv, 2023.04.06.535777. https://doi.org/10.1101/2023.04.06.535777.

46. Hobbs, S.J., Wein, T., Lu, A., Morehouse, B.R., Schnabel, J., Leavitt, A., Yirmiya, E., Sorek, R., and Kranzusch, P.J. (2022). Phage anti-CBASS and anti-Pycsar nucleases subvert bacterial immunity. Nature *605*, 522–526.

47. Huiting, E., Cao, X., Ren, J., Athukoralage, J.S., Luo, Z., Silas, S., An, N., Carion, H., Zhou, Y., Fraser, J.S., et al. (2023). Bacteriophages inhibit and evade cGAS-like immune function in bacteria. Cell *186*, 864–876.e21.

48. Chang, R.B., Toyoda, H.C., Hobbs, S.J., Richmond-Buccola, D., Wein, T., Burger, N., Chouchani, E.T., Sorek, R., and Kranzusch, P.J. (2024). A widespread family of viral sponge proteins reveals specific inhibition of nucleotide signals in anti-phage defense. bioRxiv, 2024.12.30.630793. https://doi.org/10.1101/2024.12.30.630793.

49. Jenson, J.M., Li, T., Du, F., Ea, C.-K., and Chen, Z.J. (2023). Ubiquitin-like conjugation by

bacterial cGAS enhances anti-phage defence. Nature *616*, 326–331.

50. Ho, P., Chen, Y., Biswas, S., Canfield, E., Abdolvahabi, A., and Feldman, D.E. (2023). Bacteriophage antidefense genes that neutralize TIR and STING immune responses. Cell Rep. *42*, 112305.

51. Uribe, R.V., van der Helm, E., Misiakou, M.-A., Lee, S.-W., Kol, S., and Sommer, M.O.A. (2019). Discovery and Characterization of Cas9 Inhibitors Disseminated across Seven Bacterial Phyla. Cell Host Microbe *25*, 233–241.e5.

52. Zhang, Z., Pan, S., Liu, T., Li, Y., and Peng, N. (2019). Cas4 Nucleases Can Effect Specific Integration of CRISPR Spacers. J. Bacteriol. *201*. https://doi.org/10.1128/JB.00747-18.

53. Yin, P., Zhang, Y., Yang, L., and Feng, Y. (2023). Non-canonical inhibition strategies and structural basis of anti-CRISPR proteins targeting type I CRISPR-Cas systems. J. Mol. Biol. *435*, 167996.

54. Muzyukina, P., Shkaruta, A., Guzman, N.M., Andreani, J., Borges, A.L., Bondy-Denomy, J., Maikova, A., Semenova, E., Severinov, K., and Soutourina, O. (2023). Identification of an anti-CRISPR protein that inhibits the CRISPR-Cas type I-B system in Clostridioides difficile. mSphere *8*, e0040123.

55. Katz, M.A., Sawyer, E.M., Oriolt, L., Kozlova, A., Williams, M.C., Margolis, S.R., Johnson, M., Bondy-Denomy, J., and Meeske, A.J. (2024). Diverse viral cas genes antagonize CRISPR immunity. Nature *634*, 677–683.

56. Gussow, A.B., Park, A.E., Borges, A.L., Shmakov, S.A., Makarova, K.S., Wolf, Y.I., Bondy-Denomy, J., and Koonin, E.V. (2020). Machine-learning approach expands the repertoire of anti-CRISPR protein families. Nat. Commun. *11*, 3784.

57. Wimmer, F., Englert, F., Wandera, K.G., Alkhnbashi, O.S., Collins, S.P., Backofen, R., and Beisel, C.L. (2024). Interrogating two extensively self-targeting Type I CRISPR-Cas systems in Xanthomonas albilineans reveals distinct anti-CRISPR proteins that block DNA degradation. Nucleic Acids Res. *52*, 769–783.

58. Hu, C., Myers, M.T., Zhou, X., Hou, Z., Lozen, M.L., Nam, K.H., Zhang, Y., and Ke, A. (2024). Exploiting activation and inactivation mechanisms in type I-C CRISPR-Cas3 for genome-editing applications. Mol. Cell *84*, 463–475.e5.

59. Pawluk, A., Bondy-Denomy, J., Cheung, V.H.W., Maxwell, K.L., and Davidson, A.R. (2014). A new group of phage anti-CRISPR genes inhibits the type I-E CRISPR-Cas system of Pseudomonas aeruginosa. MBio *5*, e00896.

60. Koo, J., Lee, G., Park, C., Oh, H., Hong, S.-H., Suh, J.-Y., and Bae, E. (2025). Structural and biochemical insights into the mechanism of the anti-CRISPR protein AcrIE3. Structure *33*, 160–170.e4.

61. Kim, I., Koo, J., An, S.Y., Hong, S., Ka, D., Kim, E.-H., Bae, E., and Suh, J.-Y. (2020). Structural and mechanistic insights into the CRISPR inhibition of AcrIF7. Nucleic Acids Res. *48*, 9959–9968.

62. Rauch, B.J., Silvis, M.R., Hultquist, J.F., Waters, C.S., McGregor, M.J., Krogan, N.J., and

Bondy-Denomy, J. (2017). Inhibition of CRISPR-Cas9 with bacteriophage proteins. Cell *168*, 150–158.e10.

63. Forsberg, K.J., Bhatt, I.V., Schmidtke, D.T., Javanmardi, K., Dillard, K.E., Stoddard, B.L., Finkelstein, I.J., Kaiser, B.K., and Malik, H.S. (2019). Functional metagenomics-guided discovery of potent Cas9 inhibitors in the human microbiome. Elife *8*. https://doi.org/10.7554/eLife.46540.

64. Osuna, B.A., Karambelkar, S., Mahendra, C., Christie, K.A., Garcia, B., Davidson, A.R., Kleinstiver, B.P., Kilcher, S., and Bondy-Denomy, J. (2020). Listeria phages induce Cas9 degradation to protect lysogenic genomes. Cell Host Microbe *28*, 31–40.e9.

65. Watters, K.E., Shivram, H., Fellmann, C., Lew, R.J., McMahon, B., and Doudna, J.A. (2020). Potent CRISPR-Cas9 inhibitors from Staphylococcus genomes. Proc. Natl. Acad. Sci. U. S. A. *117*, 6531–6539.

66. Mahendra, C., Christie, K.A., Osuna, B.A., Pinilla-Redondo, R., Kleinstiver, B.P., and Bondy-Denomy, J. (2020). Broad-spectrum anti-CRISPR proteins facilitate horizontal gene transfer. Nat. Microbiol. *5*, 620–629.

67. Forsberg, K.J., Schmidtke, D.T., Werther, R., Uribe, R.V., Hausman, D., Sommer, M.O.A., Stoddard, B.L., Kaiser, B.K., and Malik, H.S. (2021). The novel anti-CRISPR AcrIIA22 relieves DNA torsion in target plasmids and impairs SpyCas9 activity. PLoS Biol. *19*, e3001428.

68. Varble, A., Campisi, E., Euler, C.W., Maguin, P., Kozlova, A., Fyodorova, J., Rostøl, J.T., Fischetti, V.A., and Marraffini, L.A. (2021). Prophage integration into CRISPR loci enables evasion of antiviral immunity in Streptococcus pyogenes. Nat Microbiol *6*, 1516–1525.

69. Song, G., Tian, C., Li, J., Zhang, F., Peng, Y., Gao, X., and Tian, Y. (2023). Rapid characterization of anti-CRISPR proteins and optogenetically engineered variants using a versatile plasmid interference system. Nucleic Acids Res. *51*, 12381–12396.

70. Hynes, A.P., Rousseau, G.M., Lemay, M.-L., Horvath, P., Romero, D.A., Fremaux, C., and Moineau, S. (2017). An anti-CRISPR from a virulent streptococcal phage inhibits Streptococcus pyogenes Cas9. Nat. Microbiol. *2*, 1374–1380.

71. Hynes, A.P., Rousseau, G.M., Agudelo, D., Goulet, A., Amigues, B., Loehr, J., Romero, D.A., Fremaux, C., Horvath, P., Doyon, Y., et al. (2018). Widespread anti-CRISPR proteins in virulent bacteriophages inhibit a range of Cas9 proteins. Nat. Commun. *9*, 2919.

72. Lee, J., Mir, A., Edraki, A., Garcia, B., Amrani, N., Lou, H.E., Gainetdinov, I., Pawluk, A., Ibraheim, R., Gao, X.D., et al. (2018). Potent Cas9 Inhibition in Bacterial and Human Cells by AcrIIC4 and AcrIIC5 Anti-CRISPR Proteins. MBio *9*. https://doi.org/10.1128/mBio.02321-18.

73. Athukoralage, J.S., McMahon, S.A., Zhang, C., Grüschow, S., Graham, S., Krupovic, M., Whitaker, R.J., Gloster, T.M., and White, M.F. (2020). An anti-CRISPR viral ring nuclease subverts type III CRISPR immunity. Nature *577*, 572–575.

74. Bhoobalan-Chitty, Y., Johansen, T.B., Di Cianni, N., and Peng, X. (2019). Inhibition of type III CRISPR-Cas immunity by an Archaeal virus-encoded anti-CRISPR protein. Cell *179*,

448–458.e11.

75. Lin, J., Alfastsen, L., Bhoobalan-Chitty, Y., and Peng, X. (2023). Molecular basis for inhibition of type III-B CRISPR-Cas by an archaeal viral anti-CRISPR protein. Cell Host Microbe *31*, 1837–1849.e5.

76. Duan, N., Hand, E., Pheko, M., Sharma, S., and Emiola, A. (2024). Structure-guided discovery of anti-CRISPR and anti-phage defense proteins. Nat. Commun. *15*, 649.

77. Watters, K.E., Fellmann, C., Bai, H.B., Ren, S.M., and Doudna, J.A. (2018). Systematic discovery of natural CRISPR-Cas12a inhibitors. Science *362*, 236–239.

78. Meeske, A.J., Jia, N., Cassel, A.K., Kozlova, A., Liao, J., Wiedmann, M., Patel, D.J., and Marraffini, L.A. (2020). A phage-encoded anti-CRISPR enables complete evasion of type VI-A CRISPR-Cas immunity. Science *369*, 54–59.

79. Lin, P., Qin, S., Pu, Q., Wang, Z., Wu, Q., Gao, P., Schettler, J., Guo, K., Li, R., Li, G., et al. (2020). CRISPR-Cas13 inhibitors block RNA editing in bacteria and mammalian cells. Mol. Cell *78*, 850–861.e5.

80. Wandera, K.G., Schmelz, S., Migur, A., Kibe, A., Lukat, P., Achmedov, T., Caliskan, N., Blankenfeldt, W., and Beisel, C.L. (2025). AcrVIB1 inhibits CRISPR-Cas13b immunity by promoting unproductive crRNA binding accessible to RNase attack. Mol. Cell *85*, 1162–1175.e7.

81. Roy, D., Huguet, K.T., Grenier, F., and Burrus, V. (2020). IncC conjugative plasmids and SXT/R391 elements repair double-strand breaks caused by CRISPR-Cas during conjugation. Nucleic Acids Res. *48*, 8815–8827.

82. Cone, R., Bonura, T., and Friedberg, E.C. (1980). Inhibitor of uracil-DNA glycosylase induced by bacteriophage PBS2. Purification and preliminary characterization. J. Biol. Chem. *255*, 10354–10358.

83. Piel, D., Bruto, M., Labreuche, Y., Blanquart, F., Goudenège, D., Barcia-Cruz, R., Chenivesse, S., Le Panse, S., James, A., Dubert, J., et al. (2022). Phage-host coevolution in natural populations. Nat Microbiol *7*, 1075–1086.

84. Garb, J., Lopatina, A., Bernheim, A., Zaremba, M., Siksnys, V., Melamed, S., Leavitt, A., Millman, A., Amitai, G., and Sorek, R. (2022). Multiple phage resistance systems inhibit infection via SIR2-dependent NAD+ depletion. Nat Microbiol *7*, 1849–1856.

85. Antine, S.P., Johnson, A.G., Mooney, S.E., Leavitt, A., Mayer, M.L., Yirmiya, E., Amitai, G., Sorek, R., and Kranzusch, P.J. (2023). Structural basis of Gabija anti-phage defence and viral immune evasion. Nature. https://doi.org/10.1038/s41586-023-06855-2.

86. Dedrick, R.M., Jacobs-Sera, D., Bustamante, C.A.G., Garlena, R.A., Mavrich, T.N., Pope, W.H., Reyes, J.C.C., Russell, D.A., Adair, T., Alvey, R., et al. (2017). Prophage-mediated defence against viral attack and viral counter-defence. Nat Microbiol *2*, 16251.

87. Le, S., Wei, L., Wang, J., Tian, F., Yang, Q., Zhao, J., Zhong, Z., Liu, J., He, X., Zhong, Q., et al. (2024). Bacteriophage protein Dap1 regulates evasion of antiphage immunity and Pseudomonas aeruginosa virulence impacting phage therapy in mice. Nat. Microbiol. *9*,

1828–1841.

88. Zhao, J., Zhu, Y., Wang, C., Tian, F., Deng, J., Liao, J., Zhong, Z., Liu, J., Guo, N., Le, S., et al. (2025). Bacteriophage protein Dap2 inhibits bacterial type III secretion system and synergizes with Dap1 to evade anti-phage immunity. bioRxiv. https://doi.org/10.1101/2025.03.13.642734.

89. Kibby, E.M., Conte, A.N., Burroughs, A.M., Nagy, T.A., Vargas, J.A., Whalen, L.A., Aravind, L., and Whiteley, A.T. (2023). Bacterial NLR-related proteins protect against phage. Cell *186*, 2410–2424.e18.

90. Patel, K.M., and Seed, K.D. (2025). A Class 1 OLD family nuclease encoded by Vibrio cholerae is countered by a vibriophage-encoded direct inhibitor. bioRxivorg. https://doi.org/10.1101/2025.01.06.631583.

91. Amitsur, M., Levitz, R., and Kaufmann, G. (1987). Bacteriophage T4 anticodon nuclease, polynucleotide kinase and RNA ligase reprocess the host lysine tRNA. EMBO J. *6*, 2499–2503.

92. Murphy, K.C., Fenton, A.C., and Poteete, A.R. (1987). Sequence of the bacteriophage P22 anti-recBCD (abc) genes and properties of P22 abc region deletion mutants. Virology *160*, 456–464.

93. Murphy, K.C. (2000). Bacteriophage P22 Abc2 protein binds to RecC increases the 5' strand nicking activity of RecBCD and together with lambda bet, promotes Chi-independent recombination. J. Mol. Biol. *296*, 385–401.

94. Wilkinson, M., Wilkinson, O.J., Feyerherm, C., Fletcher, E.E., Wigley, D.B., and Dillingham, M.S. (2022). Structures of RecBCD in complex with phage-encoded inhibitor proteins reveal distinctive strategies for evasion of a bacterial immunity hub. Elife *11*. https://doi.org/10.7554/eLife.83409.

95. Sakaki, Y., Karu, A.E., Linn, S., and Echols, H. (1973). Purification and Properties of the γ-Protein Specified by Bacteriophage λ: An Inhibitor of the Host RecBC Recombination Enzyme. Proceedings of the National Academy of Sciences *70*, 2215–2219.

96. Zhang, Z., Todeschini, T.C., Wu, Y., Kogay, R., Naji, A., Rodriguez, J.C., Mondi, R., Kaganovich, D., Taylor, D.W., Bravo, J.P.K., et al. (2025). Kiwa is a bacterial membrane-embedded defence supercomplex activated by phage-induced membrane changes. bioRxivorg, 2023.02.26.530102. https://doi.org/10.1101/2023.02.26.530102.

97. Azam, A.H., Chihara, K., Kondo, K., Nakamura, T., Ojima, S., Tamura, A., Yamashita, W., Cui, L., Takahashi, Y., Watashi, K., et al. (2023). Viruses encode tRNA and anti-retron to evade bacterial immunity. bioRxiv, 2023.03.15.532788. https://doi.org/10.1101/2023.03.15.532788.

98. Carabias, A., Camara-Wilpert, S., Mestre, M.R., Lopéz-Méndez, B., Hendriks, I.A., Zhao, R., Pape, T., Fuglsang, A., Luk, S.H.-C., Nielsen, M.L., et al. (2024). Retron-Eco1 assembles NAD+-hydrolyzing filaments that provide immunity against bacteriophages. Mol. Cell *84*, 2185–2202.e12.

99. Shinedling, S., Parma, D., and Gold, L. (1987). Wild-type bacteriophage T4 is restricted by

the lambda rex genes. J. Virol. *61*, 3790–3794.

100. Belogurov, A.A., Delver, E.P., and Rodzevich, O.V. (1992). IncN plasmid pKM101 and IncI1 plasmid ColIb-P9 encode homologous antirestriction proteins in their leading regions. J. Bacteriol. *174*, 5079–5085.

101. Serfiotis-Mitsa, D., Herbert, A.P., Roberts, G.A., Soares, D.C., White, J.H., Blakely, G.W., Uhrín, D., and Dryden, D.T.F. (2010). The structure of the KlcA and ArdB proteins reveals a novel fold and antirestriction activity against Type I DNA restriction systems in vivo but not in vitro. Nucleic Acids Res. *38*, 1723–1737.

102. González-Montes, L., Del Campo, I., Garcillán-Barcia, M.P., de la Cruz, F., and Moncalián, G. (2020). ArdC, a ssDNA-binding protein with a metalloprotease domain, overpasses the recipient hsdRMS restriction system broadening conjugation host range. PLoS Genet. *16*, e1008750.

103. Belogurov, A.A., Delver, E.P., and Rodzevich, O.V. (1993). Plasmid pKM101 encodes two nonhomologous antirestriction proteins (ArdA and ArdB) whose expression is controlled by homologous regulatory sequences. J. Bacteriol. *175*, 4843–4850.

104. Meima, R., and Lidstrom, M.E. (2000). Characterization of the Minimal Replicon of a Cryptic Deinococcus radiodurans SARK Plasmid and Development of Versatile Escherichia coli-D. radiodurans Shuttle Vectors. Applied and Environmental Microbiology. https://doi.org/10.1128/aem.66.9.3856-3867.2000.

105. Dharmalingam, K., and Goldberg, E.B. (1976). Phage-coded protein prevents restriction of unmodified progeny T4 DNA. Nature *260*, 454–456.

106. Ho, C.-H., Wang, H.-C., Ko, T.-P., Chang, Y.-C., and Wang, A.H.-J. (2014). The T4 Phage DNA Mimic Protein Arn Inhibits the DNA Binding Activity of the Bacterial Histone-like Protein H-NS*. J. Biol. Chem. *289*, 27046–27054.

107. Vrielink, A., Rüger, W., Driessen, H.P., and Freemont, P.S. (1994). Crystal structure of the DNA modifying enzyme beta-glucosyltransferase in the presence and absence of the substrate uridine diphosphoglucose. EMBO J. *13*, 3413–3422.

108. Schlagman, S.L., and Hattman, S. (1983). Molecular cloning of a functional dam+ gene coding for phage T4 DNA adenine methylase. Gene *22*, 139–156.

109. Iida, S., Streiff, M.B., Bickle, T.A., and Arber, W. (1987). Two DNA antirestriction systems of bacteriophage P1, darA, and darB: characterization of darA- phages. Virology *157*, 156–166.

110. Song, H.K., Sohn, S.H., and Suh, S.W. (1999). Crystal structure of deoxycytidylate hydroxymethylase from bacteriophage T4, a component of the deoxyribonucleoside triphosphate-synthesizing complex. EMBO J. *18*, 1104–1113.

111. Piya, D., Vara, L., Russell, W.K., Young, R., and Gill, J.J. (2017). The multicomponent antirestriction system of phage P1 is linked to capsid morphogenesis. Mol. Microbiol. *105*, 399–412.

112. Teplyakov, A., Sebastiao, P., Obmolova, G., Perrakis, A., Brush, G.S., Bessman, M.J., and

Wilson, K.S. (1996). Crystal structure of bacteriophage T4 deoxynucleotide kinase with its substrates dGMP and ATP. EMBO J. *15*, 3487–3497.

113. Hutinet, G., Kot, W., Cui, L., Hillebrand, R., Balamkundu, S., Gnanakalai, S., Neelakandan, R., Carstens, A.B., Fa Lui, C., Tremblay, D., et al. (2019). 7-Deazaguanine modifications protect phage DNA from host restriction systems. Nat. Commun. *10*, 5442.

114. Drozdz, M., Piekarowicz, A., Bujnicki, J.M., and Radlinska, M. (2012). Novel non-specific DNA adenine methyltransferases. Nucleic Acids Res. *40*, 2119–2130.

115. Rifat, D., Wright, N.T., Varney, K.M., Weber, D.J., and Black, L.W. (2008). Restriction endonuclease inhibitor IPI* of bacteriophage T4: a novel structure for a dedicated target. J. Mol. Biol. *375*, 720–734.

116. Engelberg-Kulka, H., Reches, M., Narasimhan, S., Schoulaker-Schwarz, R., Klemes, Y., Aizenman, E., and Glaser, G. (1998). rexB of bacteriophage lambda is an anti-cell death gene. Proc. Natl. Acad. Sci. U. S. A. *95*, 15481–15486.

117. King, G., and Murray, N.E. (1995). Restriction alleviation and modification enhancement by the Rac prophage of Escherichia coli K-12. Mol. Microbiol. *16*, 769–777.

118. Karambelkar, S., Udupa, S., Gowthami, V.N., Ramachandra, S.G., Swapna, G., and Nagaraja, V. (2020). Emergence of a novel immune-evasion strategy from an ancestral protein fold in bacteriophage Mu. Nucleic Acids Res. *48*, 5294–5305.

119. Kahmann, R., Seiler, A., Wulczyn, F.G., and Pfaff, E. (1985). The mom gene of bacteriophage mu: a unique regulatory scheme to control a lethal function. Gene *39*, 61–70.

120. Toussaint, A. (1976). The DNA modification function of temperate phage Mu-1. Virology *70*, 17–27.

121. Loenen, W.A., and Murray, N.E. (1986). Modification enhancement by the restriction alleviation protein (Ral) of bacteriophage lambda. J. Mol. Biol. *190*, 11–22.

122. Walkinshaw, M.D., Taylor, P., Sturrock, S.S., Atanasiu, C., Berge, T., Henderson, R.M., Edwardson, J.M., and Dryden, D.T.F. (2002). Structure of Ocr from bacteriophage T7, a protein that mimics B-form DNA. Mol. Cell *9*, 187–194.

123. Studier, F.W., and Movva, N.R. (1976). SAMase gene of bacteriophage T3 is responsible for overcoming host restriction. J. Virol. *19*, 136–145.

124. Loh, S., Skurray, R., Célérier, J., Bagdasarian, M., Bailone, A., and Devoret, R. (1990). Nucleotide sequence of the psiA (plasmid SOS inhibition) gene located on the leading region of plasmids F and R6-5. Nucleic Acids Res. *18*, 4597.

125. Petrova, V., Chitteni-Pattu, S., Drees, J.C., Inman, R.B., and Cox, M.M. (2009). An SOS inhibitor that binds to free RecA protein: the PsiB protein. Mol. Cell *36*, 121–130.

126. Bagdasarian, M., Bailone, A., Angulo, J.F., Scholz, P., Bagdasarian, M., and Devoret, R. (1992). PsiB, an anti-SOS protein, is transiently expressed by the F sex factor during its transmission to an Escherichia coli K-12 recipient. Mol. Microbiol. *6*, 885–893.

127. LeRoux, M., Srikant, S., Teodoro, G.I.C., Zhang, T., Littlehale, M.L., Doron, S., Badiee, M.,

Leung, A.K.L., Sorek, R., and Laub, M.T. (2022). The DarTG toxin-antitoxin system provides phage defence by ADP-ribosylating viral DNA. Nat Microbiol *7*, 1028–1040.

128. Patel, K.M., and Seed, K.D. (2024). Sporadic phage defense in epidemic Vibrio cholerae mediated by the toxin-antitoxin system DarTG is countered by a phage-encoded antitoxin mimic. MBio *15*, e0011124.

129. Johannesman, A., Carlson, N.A., and LeRoux, M. (2024). Phages carry orphan antitoxin-like enzymes to neutralize the DarTG1 toxin-antitoxin defense system. bioRxivorg. https://doi.org/10.1101/2024.07.11.602962.

130. Alawneh, A.M., Qi, D., Yonesaki, T., and Otsuka, Y. (2016). An ADP-ribosyltransferase Alt of bacteriophage T4 negatively regulates the Escherichia coli MazF toxin of a toxin-antitoxin module. Mol. Microbiol. *99*, 188–198.

131. Otsuka, Y., and Yonesaki, T. (2012). Dmd of bacteriophage T4 functions as an antitoxin against Escherichia coli LsoA and RnlA toxins. Mol. Microbiol. *83*, 669–681.

132. Sberro, H., Leavitt, A., Kiro, R., Koh, E., Peleg, Y., Qimron, U., and Sorek, R. (2013). Discovery of functional toxin/antitoxin systems in bacteria by shotgun cloning. Mol. Cell *50*, 136–148.

133. Hilliard, J.J., Maurizi, M.R., and Simon, L.D. (1998). Isolation and characterization of the phage T4 PinA protein, an inhibitor of the ATP-dependent lon protease of Escherichia coli. J. Biol. Chem. *273*, 518–523.

134. Srikant, S., Guegler, C.K., and Laub, M.T. (2022). The evolution of a counter-defense mechanism in a virus constrains its host range. Elife *11*. https://doi.org/10.7554/eLife.79549.

135. Azulay, G., Sigal, N., Tzohar Rabinovich, K., Koenigsfeld, D., Stadnyuk, O., Das, A., Lisitzin, P., Biderman, E., Borovok, I., and Herskovits, A.A. (2025). A prophage-encoded anti-phage defense system that prevents phage DNA packaging by targeting the terminase complex. bioRxiv. https://doi.org/10.1101/2025.02.27.640495.

136. Yamashita, W., Chihara, K., Azam, A.H., Kondo, K., Ojima, S., Tamura, A., Imanaka, M., Nobrega, F.L., Takahashi, Y., Watashi, K., et al. (2025). Phage engineering to overcome bacterial Tmn immunity in Dhillonvirus. Commun. Biol. *8*, 290.

137. Azulay, G., Pasechnek, A., Stadnyuk, O., Ran-Sapir, S., Fleisacher, A.M., Borovok, I., Sigal, N., and Herskovits, A.A. (2022). A dual-function phage regulator controls the response of cohabiting phage elements via regulation of the bacterial SOS response. Cell Rep. *39*, 110723.

138. Bhoobalan-Chitty, Y., Xu, S., Martinez-Alvarez, L., Karamycheva, S., Makarova, K.S., Koonin, E.V., and Peng, X. (2024). Regulatory sequence-based discovery of anti-defense genes in archaeal viruses. Nat. Commun. *15*, 3699.

139. Tesson, F., Huiting, E., Wei, L., Ren, J., Johnson, M., Planel, R., Cury, J., Feng, Y., Bondy-Denomy, J., and Bernheim, A. (2024). Exploring the diversity of anti-defense systems across prokaryotes, phages and mobile genetic elements. Nucleic Acids Res., gkae1171.

140. Yan, Y., Zheng, J., Zhang, X., and Yin, Y. (2024). dbAPIS: a database of anti-prokaryotic immune system genes. Nucleic Acids Res. *52*, D419–D425.

141. Dong, C., Hao, G.-F., Hua, H.-L., Liu, S., Labena, A.A., Chai, G., Huang, J., Rao, N., and Guo, F.-B. (2018). Anti-CRISPRdb: a comprehensive online resource for anti-CRISPR proteins. Nucleic Acids Res. *46*, D393–D398.

142. Dong, C., Wang, X., Ma, C., Zeng, Z., Pu, D.-K., Liu, S., Wu, C.-S., Chen, S., Deng, Z., and Guo, F.-B. (2022). Anti-CRISPRdb v2.2: an online repository of anti-CRISPR proteins including information on inhibitory mechanisms, activities and neighbors of curated anti-CRISPR proteins. Database (Oxford) *2022*, baac010.

143. Wang, J., Dai, W., Li, J., Li, Q., Xie, R., Zhang, Y., Stubenrauch, C., and Lithgow, T. (2021). AcrHub: an integrative hub for investigating, predicting and mapping anti-CRISPR proteins. Nucleic Acids Res. *49*, D630–D638.

144. Burley, S.K., Bhikadiya, C., Bi, C., Bittrich, S., Chao, H., Chen, L., Craig, P.A., Crichlow, G.V., Dalenberg, K., Duarte, J.M., et al. (2023). RCSB Protein Data Bank (RCSB.org): delivery of experimentally-determined PDB structures alongside one million computed structure models of proteins from artificial intelligence/machine learning. Nucleic Acids Res. *51*, D488–D508.

145. O'Brien, R.E., Santos, I.C., Wrapp, D., Bravo, J.P.K., Schwartz, E.A., Brodbelt, J.S., and Taylor, D.W. (2020). Structural basis for assembly of non-canonical small subunits into type I-C Cascade. Nat. Commun. *11*, 5931.

146. Lu, M., Yu, C., Zhang, Y., Ju, W., Ye, Z., Hua, C., Mao, J., Hu, C., Yang, Z., and Xiao, Y. (2024). Structure and genome editing of type I-B CRISPR-Cas. Nat. Commun. *15*, 4126.

147. Lee, Y.-J., Dai, N., Walsh, S.E., Müller, S., Fraser, M.E., Kauffman, K.M., Guan, C., Corrêa, I.R., Jr, and Weigele, P.R. (2018). Identification and biosynthesis of thymidine hypermodifications in the genomic DNA of widespread bacterial viruses. Proc. Natl. Acad. Sci. U. S. A. *115*, E3116–E3125.

148. Zhao, G., Chen, C., Xiong, W., Gao, T., Deng, Z., Wu, G., and He, X. (2016). Structural basis of the substrate preference towards CMP for a thymidylate synthase MilA involved in mildiomycin biosynthesis. Sci. Rep. *6*, 39675.

149. Burman, N., Belukhina, S., Depardieu, F., Wilkinson, R.A., Skutel, M., Santiago-Frangos, A., Graham, A.B., Livenskyi, A., Chechenina, A., Morozova, N., et al. (2024). A virally encoded tRNA neutralizes the PARIS antiviral defence system. Nature *634*, 424–431.

150. Dot, E.W., Thomason, L.C., and Chappie, J.S. (2023). Everything OLD is new again: How structural, functional, and bioinformatic advances have redefined a neglected nuclease family. Mol. Microbiol. *120*, 122–140.

151. Shu, X., Wang, R., Cheng, F., Li, Z., Wu, A., Xue, Q., Liu, C., Cao, X., Feng, Y., and Li, M. (2024). CRISPR-Cas supervises diverse anti-phage defense systems. bioRxiv, 2024.12.27.630466. https://doi.org/10.1101/2024.12.27.630466.

152. Nomburg, J., Doherty, E.E., Price, N., Bellieny-Rabelo, D., Zhu, Y.K., and Doudna, J.A. (2024). Birth of protein folds and functions in the virome. Nature *633*, 710–717.

153. Cohen, D., Melamed, S., Millman, A., Shulman, G., Oppenheimer-Shaanan, Y., Kacen, A., Doron, S., Amitai, G., and Sorek, R. (2019). Cyclic GMP-AMP signalling protects bacteria against viral infection. Nature *574*, 691–695.

154. Bähre, H., Hartwig, C., Munder, A., Wolter, S., Stelzer, T., Schirmer, B., Beckert, U., Frank, D.W., Tümmler, B., Kaever, V., et al. (2015). cCMP and cUMP occur in vivo. Biochem. Biophys. Res. Commun. *460*, 909–914.

155. Hobbs, S.J., and Kranzusch, P.J. (2024). Nucleotide immune signaling in CBASS, Pycsar, Thoeris, and CRISPR antiphage defense. Annu. Rev. Microbiol. *78*. https://doi.org/10.1146/annurev-micro-041222-024843.

156. Seifert, R. (2017). CCMP and cUMP across the tree of life: From cCMP and cUMP generators to cCMP- and cUMP-regulated cell functions. Handb. Exp. Pharmacol. *238*, 3–23.

157. Schargel, R.D., Qayyum, M.Z., Tanwar, A.S., Kalathur, R.C., and Kellogg, E.H. (2024). Structure of Fanzor2 reveals insights into the evolution of the TnpB superfamily. Nat. Struct. Mol. Biol., 1–4.

158. Nair, P.A., Nandakumar, J., Smith, P., Odell, M., Lima, C.D., and Shuman, S. (2007). Structural basis for nick recognition by a minimal pluripotent DNA ligase. Nat. Struct. Mol. Biol. *14*, 770–778.

159. Sriskanda, V., Schwer, B., Ho, C.K., and Shuman, S. (1999). Mutational analysis of Escherichia coli DNA ligase identifies amino acids required for nick-ligation in vitro and for in vivo complementation of the growth of yeast cells deleted for CDC9 and LIG4. Nucleic Acids Res. *27*, 3953–3963.

160. Ho, C.K., Van Etten, J.L., and Shuman, S. (1997). Characterization of an ATP-dependent DNA ligase encoded by Chlorella virus PBCV-1. J. Virol. *71*, 1931–1937.

161. Chen, Y., Liu, H., Yang, C., Gao, Y., Yu, X., Chen, X., Cui, R., Zheng, L., Li, S., Li, X., et al. (2019). Structure of the error-prone DNA ligase of African swine fever virus identifies critical active site residues. Nat. Commun. *10*, 387.

162. Pereira-Lopes, S., Celhar, T., Sans-Fons, G., Serra, M., Fairhurst, A.-M., Lloberas, J., and Celada, A. (2013). The exonuclease Trex1 restrains macrophage proinflammatory activation. J. Immunol. *191*, 6128–6135.

163. Kawane, K., Tanaka, H., Kitahara, Y., Shimaoka, S., and Nagata, S. (2010). Cytokine-dependent but acquired immunity-independent arthritis caused by DNA escaped from degradation. Proc. Natl. Acad. Sci. U. S. A. *107*, 19432–19437.

164. Hao, S., Zheng, X., Zhu, Y., Yao, Y., Li, S., Xu, Y., and Feng, W.-H. (2023). African swine fever virus QP383R dampens type I interferon production by promoting cGAS palmitoylation. Front. Immunol. *14*, 1186916.

165. Kerr, S.M., Johnston, L.H., Odell, M., Duncan, S.A., Law, K.M., and Smith, G.L. (1991). Vaccinia DNA ligase complements Saccharomyces cerevisiae cdc9, localizes in cytoplasmic factories and affects virulence and virus sensitivity to DNA damaging agents. EMBO J. *10*, 4343–4350.

166. Zhou, W., Richmond-Buccola, D., Wang, Q., and Kranzusch, P.J. (2022). Structural basis of human TREX1 DNA degradation and autoimmune disease. Nat. Commun. *13*, 4277.

167. Chan, M.P., Onji, M., Fukui, R., Kawane, K., Shibata, T., Saitoh, S.-I., Ohto, U., Shimizu, T., Barber, G.N., and Miyake, K. (2015). DNase II-dependent DNA digestion is required for DNA sensing by TLR9. Nat. Commun. *6*, 5853.

168. Yan, N., Regalado-Magdos, A.D., Stiggelbout, B., Lee-Kirsch, M.A., and Lieberman, J. (2010). The cytosolic exonuclease TREX1 inhibits the innate immune response to human immunodeficiency virus type 1. Nat. Immunol. *11*, 1005–1013.

169. Brzostek-Racine, S., Gordon, C., Van Scoy, S., and Reich, N.C. (2011). The DNA damage response induces IFN. J. Immunol. *187*, 5336–5345.

170. Morales, A.J., Carrero, J.A., Hung, P.J., Tubbs, A.T., Andrews, J.M., Edelson, B.T., Calderon, B., Innes, C.L., Paules, R.S., Payton, J.E., et al. (2017). A type I IFN-dependent DNA damage response regulates the genetic program and inflammasome activation in macrophages. Elife *6*. https://doi.org/10.7554/eLife.24655.

171. Berman, H.M., Westbrook, J., Feng, Z., Gilliland, G., Bhat, T.N., Weissig, H., Shindyalov, I.N., and Bourne, P.E. (2000). The Protein Data Bank. Nucleic Acids Res. *28*, 235–242.

172. Seo, H., Kim, S., Sagong, H.-Y., Son, H.F., Jin, K.S., Kim, I.-K., and Kim, K.-J. (2016). Structural basis for cytokinin production by LOG from Corynebacterium glutamicum. Sci. Rep. *6*, 31390.

173. Quevillon-Cheruel, S., Campo, N., Mirouze, N., Mortier-Barrière, I., Brooks, M.A., Boudes, M., Durand, D., Soulet, A.-L., Lisboa, J., Noirot, P., et al. (2012). Structure-function analysis of pneumococcal DprA protein reveals that dimerization is crucial for loading RecA recombinase onto DNA during transformation. Proc. Natl. Acad. Sci. U. S. A. *109*, E2466–E2475.

174. Govande, A.A., Duncan-Lowey, B., Eaglesham, J.B., Whiteley, A.T., and Kranzusch, P.J. (2021). Molecular basis of CD-NTase nucleotide selection in CBASS anti-phage defense. Cell Rep. *35*, 109206.

175. Eddy, S.R. (1998). Profile hidden Markov models. Bioinformatics *14*, 755–763.

176. Paysan-Lafosse, T., Andreeva, A., Blum, M., Chuguransky, S.R., Grego, T., Pinto, B.L., Salazar, G.A., Bileschi, M.L., Llinares-López, F., Meng-Papaxanthos, L., et al. (2025). The Pfam protein families database: embracing AI/ML. Nucleic Acids Res. *53*, D523–D534.

177. Abramson, J., Adler, J., Dunger, J., Evans, R., Green, T., Pritzel, A., Ronneberger, O., Willmore, L., Ballard, A.J., Bambrick, J., et al. (2024). Accurate structure prediction of biomolecular interactions with AlphaFold 3. Nature *630*, 493–500.

178. van Kempen, M., Kim, S.S., Tumescheit, C., Mirdita, M., Lee, J., Gilchrist, C.L.M., Söding, J., and Steinegger, M. (2023). Fast and accurate protein structure search with Foldseek. Nat. Biotechnol. https://doi.org/10.1038/s41587-023-01773-0.

179. Moffat, L., and Jones, D.T. (2021). Increasing the accuracy of single sequence prediction methods using a deep semi-supervised learning framework. Bioinformatics *37*, 3744–3751.

180. Egorov, A.A., Hauryliuk, V., and Atkinson, G.C. (2024). Systematic annotation of hyper-variability hotspots in phage genomes and plasmids. bioRxiv, 2024.10.15.618418. https://doi.org/10.1101/2024.10.15.618418.

181. Sayers, E.W., Cavanaugh, M., Clark, K., Ostell, J., Pruitt, K.D., and Karsch-Mizrachi, I. (2020). GenBank. Nucleic Acids Res. *48*, D84–D86.

182. Camargo, A.P., Nayfach, S., Chen, I.-M.A., Palaniappan, K., Ratner, A., Chu, K., Ritter, S.J., Reddy, T.B.K., Mukherjee, S., Schulz, F., et al. (2023). IMG/VR v4: an expanded database of uncultivated virus genomes within a framework of extensive functional, taxonomic, and ecological metadata. Nucleic Acids Res. *51*, D733–D743.

183. Altschul, S.F., Gish, W., Miller, W., Myers, E.W., and Lipman, D.J. (1990). Basic local alignment search tool. J. Mol. Biol. *215*, 403–410.

184. Steinegger, M., and Söding, J. (2017). MMseqs2 enables sensitive protein sequence searching for the analysis of massive data sets. Nat. Biotechnol. *35*, 1026–1028.

185. Steinegger, M., and Söding, J. (2018). Clustering huge protein sequence sets in linear time. Nat. Commun. *9*, 2542.

186. Di Tommaso, P., Chatzou, M., Floden, E.W., Barja, P.P., Palumbo, E., and Notredame, C. (2017). Nextflow enables reproducible computational workflows. Nat. Biotechnol. *35*, 316–319.

187. Salazar, G.A., Luciani, A., Watkins, X., Kandasaamy, S., Rice, D.L., Blum, M., Bateman, A., and Martin, M. (2023). Nightingale: web components for protein feature visualization. Bioinform. Adv. *3*, vbad064.

188. Boratyn, G.M., Camacho, C., Cooper, P.S., Coulouris, G., Fong, A., Ma, N., Madden, T.L., Matten, W.T., McGinnis, S.D., Merezhuk, Y., et al. (2013). BLAST: a more efficient report with usability improvements. Nucleic Acids Res. *41*, W29–W33.

189. Azam, A.H., Kondo, K., Chihara, K., Nakamura, T., Ojima, S., Nie, W., Tamura, A., Yamashita, W., Sugawara, Y., Sugai, M., et al. (2024). Evasion of antiviral bacterial immunity by phage tRNAs. Nat. Commun. *15*, 9586.

190. Tesson, F., Planel, R., Egorov, A.A., Georjon, H., Vaysset, H., Brancotte, B., Néron, B., Mordret, E., Atkinson, G.C., Bernheim, A., et al. (2024). A comprehensive resource for exploring antiphage defense: DefenseFinder webservice,wiki and databases. Peer Community J. *4*. https://doi.org/10.24072/pcjournal.470.

191. Bryant, P., Pozzati, G., and Elofsson, A. (2022). Improved prediction of protein-protein interactions using AlphaFold2. Nat. Commun. *13*, 1265.

192. Tesson, F., Hervé, A., Mordret, E., Touchon, M., d'Humières, C., Cury, J., and Bernheim, A. (2022). Systematic and quantitative view of the antiviral arsenal of prokaryotes. Nat. Commun. *13*, 2561.

193. Cock, P.J.A., Antao, T., Chang, J.T., Chapman, B.A., Cox, C.J., Dalke, A., Friedberg, I., Hamelryck, T., Kauff, F., Wilczynski, B., et al. (2009). Biopython: freely available Python tools for computational molecular biology and bioinformatics. Bioinformatics *25*, 1422–1423.

194. Goldfarb, T., Kodali, V.K., Pujar, S., Brover, V., Robbertse, B., Farrell, C.M., Oh, D.-H., Astashyn, A., Ermolaeva, O., Haddad, D., et al. (2025). NCBI RefSeq: reference sequence standards through 25 years of curation and annotation. Nucleic Acids Res. *53*, D243–D257.

195. Couvin, D., Bernheim, A., Toffano-Nioche, C., Touchon, M., Michalik, J., Néron, B., Rocha, E.P.C., Vergnaud, G., Gautheret, D., and Pourcel, C. (2018). CRISPRCasFinder, an update of CRISRFinder, includes a portable version, enhanced performance and integrates search for Cas proteins. Nucleic Acids Res. *46*, W246–W251.

196. UniProt Consortium (2025). UniProt: The universal protein knowledgebase in 2025. Nucleic Acids Res. *53*, D609–D617.

197. Jurrus, E., Engel, D., Star, K., Monson, K., Brandi, J., Felberg, L.E., Brookes, D.H., Wilson, L., Chen, J., Liles, K., et al. (2018). Improvements to the APBS biomolecular solvation software suite. Protein Sci. *27*, 112–128.

198. Huo, Y., Nam, K.H., Ding, F., Lee, H., Wu, L., Xiao, Y., Farchione, M.D., Jr, Zhou, S., Rajashankar, K., Kurinov, I., et al. (2014). Structures of CRISPR Cas3 offer mechanistic insights into Cascade-activated DNA unwinding and degradation. Nat. Struct. Mol. Biol. *21*, 771–777.

199. Wang, S., Gabel, C., Siddique, R., Klose, T., and Chang, L. (2023). Molecular mechanism for Tn7-like transposon recruitment by a type I-B CRISPR effector. Cell *186*, 4204–4215.e19.

200. Nishimasu, H., Ran, F.A., Hsu, P.D., Konermann, S., Shehata, S.I., Dohmae, N., Ishitani, R., Zhang, F., and Nureki, O. (2014). Crystal structure of Cas9 in complex with guide RNA and target DNA. Cell *156*, 935–949.

201. Seo, H., and Kim, K.-J. (2017). Structural basis for a novel type of cytokinin-activating protein. Sci. Rep. *7*, 45985.

202. Li, Z., Jaroszewski, L., Iyer, M., Sedova, M., and Godzik, A. (2020). FATCAT 2.0: towards a better understanding of the structural diversity of proteins. Nucleic Acids Res. *48*, W60–W64.

METHOD DETAILS

Data collection

We analysed research literature reporting phage ADPs and extracted information on the defence systems they counteract, mechanisms of action, PDB accessions, data on their potential to trigger other defence systems, and protein sequences. We did not include entries where protein sequences were not provided in the articles, supplementary material or as identifiers in protein databases. For ADPs that function as part of multicomponent systems, we collected and cross-referenced relevant entries accordingly. Additionally, we assigned Evidence and Conclusion Ontology (ECO)[5] labels to describe evidence supporting entries in our database. We categorised entries in our database based on MoA.

We ran hmmer v3.4[175] (with option --cut_ga) with Pfam 37.3[176] to identify existing profile HMMs in Pfam corresponding to ADPs. We produced structural models using AlphaFold 3[177] for ADPs without a corresponding entry in the PDB. We used AlphaFold 3 v3.0.1 and generated four seeds (1, 2, 3 and 4) through this work. For ADPs without characterised MoA, we searched for structural homolog using FoldSeek[178] in the pregenerated target databases bundled with FoldSeek (PDB, Alphafold/UniProt and ESMAtlas30). We used S4PRED to predict protein secondary structure based on the ADP sequences[179]. We used FoldSeek release 10-941cd33 and the following command for the identification of homologous structures through this work: *foldseek easy-search* [query_structure] [target_database] [output_file].

Diversity hotspots are genomic regions characterized by elevated variability, typically flanked by conserved genes, and frequently observed in phage and plasmid genomes. These regions arise through mechanisms such as mobile genetic element insertions, recombination, and hypermutation, and often carry accessory genes involved in defence, anti-defence, virulence, and antimicrobial resistance[180]. We ran iLund4u to identify ADPs encoded such diversity hotspots in phages (*ilund4u protein -fa* [adp].fa *-db* phages *-o* [adp]_phages) and plasmids[180](*ilund4u protein -fa* [adp].fa *-db* plasmid *-o* [adp]_plasmid) using the default parameters. These results may be used to identify candidate anti-defence genes, as there is a notion that anti-defence genes are co-localised within phage genomes.

We downloaded three databases to identify homologs of ADPs: (i) the GenBank database of phage genomes (release from 30-04-2025)[181], (ii) the GenBank database of viral genomes (release from 30-04-2025), and (iii) IMG/VR version 7.1[182]. We used BLASTp (v2.12.0+)[183] searches to identify homologs, applying the following criteria to determine significance: e-value < 1e-5, query coverage ≥ 80%, and identity ≥ 30%. Additionally, we extracted available phylogenetic information about genomes encoding homologs of ADPs using python package ete3 (v.3.1.3).

Comparison with other resources

To compare ADP coverage in EVADES, dbAPIS[140], and Anti-Defense Finder[139], we combined all sequences from these databases, dereplicated them using MMseqs2 (v13.45111, --cov-mode 0)[184,185] at 90% identity and 90% coverage, and assessed the presence of sequences or closely related homologs (defined as sequences sharing 90% identity over 90% of the query length) in all three databases. Additionally, we calculated the number of ADPs in per bacterial defense family and aggregated the results to assess how well EVADES, dbAPIS, and Anti-Defense Finder represent the diversity of ADPs.

Creation of the web resource

The web resource was developed using the Python Django framework, and the presented data and metadata are stored in an SQLite database. We created a Nextflow[186] pipeline to automate SQLite database generation from a json-file with the database. For the visualisations, the following JavaScript libraries were utilised: pdbe-molstar v3.1.0 for the 3D structure viewer, feature-viewer@v1.1.0 for the predicted secondary structure viewer, jQuery DataTables for Pfam annotations, and the Nightingale library[187] for the interactive Pfam annotations viewer.

Sequence similarity comparison

We generated a BLASTP database from all ADP sequences, we conducted homology searches using individual ADP sequences as queries and an e-value threshold of 0.001, and filtered out self-matches. All sequence pairs, except for two (Lidtsur 6 - Forsur 7 and AcrIIA1 - AcrIB5), exceeded the empirical threshold of 25% identity used to establish homology. To further investigate these exceptions, we used FATCAT 2.0 to assess structural similarity. We used the local version of FATCAT 2.0 and the following command for all pairwise structure similarity comparisons throughout this work: FATCAT -p1 [pdb_file_1] -p2 [pdb_file_1] -o [pdb_file_1-pdb_file_2] -m -ac -t The resulting p-values were: 4.65e-12 for Lidtsur 6 - Forsur 7 and 4.38e-07 for AcrIIA1 - AcrIB5, so we included them as pairs sharing homology.

Similarity with the defence trigger

We compared ADP sequences from our collection with the triggers of bacterial defence systems[25] using BLASTP (e-value < 0.001)[188]. Among the matches, we focused on the Avs type I trigger (NCBI GenPept accession: WP_317906625.1) from *Bacillus* phage SBSphiC, as it was not reported as ADP, and predicted its 3D structure using AlphaFold 3 using the same parameters as previously specified[177], and searched for homologs in PDB[171] using FoldSeek[178]. The closest homolog identified was CMP hydroxymethylase MilA (PDB accession: 5JNH). We aligned the structure of MilA with the Avs type I trigger using the local version of FATCAT 2.0 (p-value 0.00e+00). Residues K133 and A176 define MilA's substrate specificity; it has been shown that the mutations K133R and A176S change substrate specificity from CMP to dCMP[148]. We analysed the alignment between the Avs type I trigger and CMP hydroxymethylase MilA in Pymol (version 3.1.4.1, used throughout this work), identifying the closest residues in the Avs type I trigger that align with those determining substrate specificity in MilA.

It has previously been demonstrated that Bacillus phage SP10, which is closely related to SBSphiC, encodes a dUMP hydroxymethylase involved in DNA hypermodification[147] (NCBI GenPept accession: YP_007003445.1), which shares 97% sequence identity with the Avs type I trigger. This suggested that dUMP may also serve as a substrate of the type I Avs trigger. To explore this, we co-folded the Avs type I trigger with dUMP, dCMP, and CMP using AlphaFold 3[177], as ipTM scores for complexes can be indicative of the substrate preference.

Prediction of ADPs inhibiting multiple defence systems based on protein sharing network for defence systems

We compiled information from research articles on defence proteins known to interact directly with ADPs. Although direct interactions between anti-Septu proteins (Anhur and Svarog[15]) and the Septu proteins have not been reported, we included PtuA and PtuB in our analysis due to their presence and conservation between Septu defence and type 1A retrons (Ec78, Ec83, Vc95)[189]. Some ADPs with uncharacterised MoA inhibit defence systems composed of a single protein, suggesting that those defence proteins are likely to be targeted—directly or indirectly—by ADPs. Therefore, we also included these defence proteins in our analysis. A full list of the defence proteins used in this experiment is provided in Supplementary Table 2.

We retrieved the structures of these defence proteins from DefenseFinder[190] (monomer structures) and the PDB, or predicted them if not available in either source. All monomer structures available in DefenseFinder[190] were included and supplemented with structures of defence proteins from the previous experiment (see Supplementary Table 2) to build a reference database of defence proteins. We used the command *foldseek createdb*[178] to construct the

target database. Structural homologues of ADP-binding proteins were identified using *foldseek easy-search*[178], applying a stringent e-value cut-off (<1e-8) to prioritise functionally relevant structural matches. We then merged the resulting tables, removed redundancy (e.g. multiple entries for the same protein across different defence system subtypes), and visualised the results using the Pyvis 0.3.2 library in Python.

To validate selected structural matches, we used AlphaFold 3 to predict complex formation, with a particular focus on interactions between PglX homologs and Ocr. First, we predicted the structure of the PglX-Ocr complex and assessed whether the ipTM score exceeded the recommended threshold of 0.6. We also predicted interactions between Ocr and four other defence proteins: gp28 (Panchino), drmMII (DISARM), Ecoprrl (RM), and HsdM (RM). While predictions for Ecoprrl (ipTM = 0.42, pTM = 0.75) and HsdM (ipTM = 0.3, pTM = 0.72) did not meet the threshold, AlphaFold 3 produced moderate-confidence predictions for the Ocr–gp28 complex (ipTM = 0.79, pTM = 0.79, pDockQ = 0.56) and the Ocr–drmMII complex (ipTM = 0.72, pTM = 0.87, pDockQ = 0.401). To calculate the pDockQ score, we implemented a custom script capable of processing cif-files generated by AlphaFold 3. The pDockQ metric was proposed by Bryant et al.[191] as a measure of protein-protein complex prediction quality, with a recommended threshold of pDockQ ≥ 0.23. We visualised both predicted complexes in PyMOL, highlighting residues in gp28 and drmMII that interact with Ocr, defined as residues within 8 Å of any Ocr residue.

Prediction of direct interactions between ADPs with uncharacterised mechanism of action and corresponding defence systems

First, we obtained the sequences of the defence systems which were inhibited by uncharacterised proteins. We downloaded all monomer PDB-files provided by the DefenseFinder database[190,192], converted them to fasta-format using BioPython 1.79[193], and removed duplicate entries. As sequences for CRISPR and RM proteins were absent from the DefenseFinder database, we searched for them in RefSeq[194], CRISPRCasFinder[195], UniProt[196] and PDB[144]. We looked for defence protein sequences with taxonomic annotations corresponding to species specified in the original papers reporting ADPs. We excluded the O-antigen-based barrier, as the polysaccharide chains are highly variable and cannot be reliably modelled. We also excluded ADPs with uncharacterised MoA shown to act indirectly—such as ArdB and KlcA—or are hypothesised to act as negative regulators of anti-defence systems (e.g. ArdK, ArdR, and DdrB). The complete table of sequences for co-folding experiments is provided in Supplementary Table 3. Secondly, we run the AlphaFold 3[177] v3.0.1 data pipeline (*--run_inference=false*) on individual defence and anti-defence protein sequences to generate MSA and structural templates. This approach allowed reuse of MSA/template data for proteins appearing multiple times. Third, we created JSON files combining the MSAs and templates from the previous step for each corresponding defence and anti-defence protein pair. We then ran AlphaFold 3[177] inference with 4 seeds (1, 2, 3, 4), producing 20 models and focused only on those complexes where both the average ipTM and the best model's ipTM were greater than 0.6. We then computed the pDockQ scores for the best models. Predicted complexes were classified into high-confidence (best model ipTM ≥ 0.8) and moderate-confidence (0.6 < best model ipTM < 0.8). All results are available in Supplementary Table 4.

Putative MoA for AcrIC5

We predicted a high-confidence (ipTM = 0.92, pTM = 0.85, pDockQ = 0.56) complex between AcrIC5 and Pseudomonas aeruginosa Cas8c (PaCas8c, NCBI GenPept accession: UEM35121.1). To gain mechanistic insights from the predicted complex between AcrIC5 and PaCas8c, we sought to annotate the region in Cas8c that binds AcrIC5. We looked for the closest homolog in the PDB using FoldSeek[178] and found a Cascade complex containing a Cas8c homolog from Desulfovibrio vulgaris (PDB accession: 7KHA)[145]. We aligned it using FATCAT 2.0 with the structure of PaCas8c predicted with AlphaFold 3[177] and found that the binding site for AcrIC5 is extensive and includes the putative PAM-binding site (residues: GVDAKGK). We visualised the results in Pymol, colouring AcrIC5 based on electrostatic potential (using APBS Electrostatics module[197]).

Putative MoA for AcrIC3

We predicted a high-confidence complex (ipTM = 0.91, pTM = 0.90, pDockQ = 0.633) between AcrIC3 and Pseudomonas aeruginosa Cas3 (PaCas3, NCBI GenPept: UEM35119.1). To annotate PaCas3 protein, we took its structure predicted by AlphaFold 3[177] and looked for structural homologs in PDB using FoldSeek[178] . We identified Cas3 from Thermobifida fusca YX (PDB accession: 4QQZ) as a closest homolog (e-value 1.74e-18)[198]. Then we aligned the structures using FATCAT 2.0, and relying on the domain coordinates reported for *Thermobifida fusca'*s Cas, annotated domains (1-216 HD, 217-430 RecA1, 431-602 RecA2, 603-649 Linker, and 650-744 CTD) in PaCas3. We visualised the complex between AcrIC3 and PaCas3 in Pymol. We used the BioPython 1.79[193] module NeighborSearch to identify residues in Cas3 likely interacting with residues in AcrIC3 (defined as residues in 8Å or less). We used matplotlib (v.3.4.3) to visualise the domain architecture, plotting grey dots on residues in PaCas3 interacting with AcrIC3.

Putative MoA for AcrIB4

We predicted a high-confidence complex (ipTM = 0.91, pTM = 0.76, pDockQ = 0.424) between AcrIB4 and Listeria seeligeri Cas8 (LsCas8b1) with its N-terminal residues (504–530) forming the binding interface. To annotate the LsCas8b1 binding interface, we took its AlphaFold 3[177] predicted structure and looked for structural homologs in the PDB using FoldSeek[178] . However, as we did not identify any matches, we manually looked for type I-B Cascade complexes containing Cas8 in the PDB and found a complex (PDB accession: 8FCJ) where Cas8 protein shares high similarity to LsCas8b1[199]. We found that the Cas8 residues corresponding to the AcrIB4 binding interface in LsCas8b1 are involved in binding Cas11 in the type I-B Cascade. We visualised the complexes between AcrIB4-LsCas8b1 and Cas8-Cas11 in PyMol.

Putative MoA for AcrIIA26

We predicted a high-confidence complex (ipTM = 0.87, pTM = 0.79, pDockQ = 0.634) between AcrIIA26 and SpyCas9 (NCBI GenPept accession: QHB64844.1). We wanted to explore the positioning of AcrIIA26 relative to sgRNA and target DNA, so we took sgRNA and target DNA sequences from a PDB entry with accession 4OO8[200], co-folded them with SpyCas9 using AlphaFold 3[177] and predicted a very high-confidence complex (ipTM = 0.94, pTM = 0.92). We positioned the AcrIIA26-SpyCas9 complex and the complex between sgRNA, target DNA and SpyCas9 similarly in space using PyMol, which allowed us to infer that AcrIIA26 occludes the

DNA binding site. We calculated electrostatic potential on AcrIIA26 using APBS Electrostatics module in PyMol and visualised its surface interacting with SpyCas9.

Structure based search for anti-defence proteins in eukaryotic viral protein database

We conducted structure-based homology search for phage ADPs in a eukaryotic viral protein database[152] using FoldSeek[178] (considering the size of DB, 68K entries, we filtered on e-value < 0.00001). Then, we analysed the results and focused on matches with ADPs counteracting defence systems shared between bacteria and eukaryotes, namely anti-Avs proteins ORF83 and ORF55[14] and NTase[50] inhibiting TIR and STING immune response.

ORF55 functional annotation and homologs in eukaryotic viruses

We looked for homologs of ORF55 using its structural model in PDB [144] with FoldSeek[178] and found that the closest match is the DNA ligase (PDB accession: 2Q2U) from Chlorella virus (eukaryotic DNA viruses). We superimposed ORF55 and the DNA ligase from Chlorella virus using FATCAT 2.0 (p-value = 0.00e+00). We modelled interaction between ORF55 and the DNA fragment from the Chlorella virus DNA ligase using AlphaFold 3[177] and predicted a high confidence complex. We analysed the paper reporting the structure of the DNA ligase from the Chlorella virus and retrieved active site residues responsible for its catalytic activity. Then we superimposed ORF55 structure with the Chlorella virus DNA ligase using FATCAT 2.0 and analysed the alignment in Pymol, and retrieved the residues in ORF55 aligning with the active site residues in the Chlorella virus DNA ligase. Next we used the same DNA fragment, but introduced a nick, and one- and two-nucleotide gapes and co-folded with ORF55 and ATP, where similar to the Chlorella virus DNA ligase, ORF55 showed preference for nicked (ipTM = 0.95, pTM = 0.95) and one-nucleotide gapped DNA (ipTM = 0.95, pTM = 0.95) compared to two-nucleotide gapped DNA (ipTM = 0.87, pTM = 0.91).

ORF83 functional annotation and homologs in eukaryotic viruses

We looked for structural homologs of ORF83 in the PDB database using FoldSeek[178] , aligned the top four matches using FATCAT 2.0 and identified Cg1261 (PDB ID: 5WQ3, 4.39e-7) – the type II cytokine activating protein from LOG family (The Lonely Guy) as the highest scoring match. We analysed the paper with functional characterisation of Cg1261 and found it was reported to hydrolyze AMP into an adenine base and ribose 5-phosphate. So, we modelled interaction between ORF83 and AMP using AlphaFold 3[177]. Then we aligned the ORF83-AMP complex with Cg1261 using FATCAT 2.0, selected active site residues in Cg1261 from the paper[201] and found closest aligning residues in ORF83. Then we predicted the structure of ORF83's homolog from eukaryotic dsDNA viruses (NCBI GenPept accession: YP_009506880) in complex with AMP, aligned it with ORF83 using FATCAT 2.0, and visualised the results in Pymol.

NTase

We aligned the structural model of *Bacillus* phage Bcp1 NTase with its homolog we identified in *Erinnyis ello* granulovirus (NCBI GenPept accession: YP_009091875.1) using FATCAT 2.0[202] and visualised the results in Pymol. Next, we calculated the number of positions in the phage NTase and its homolog from *Erinnyis ello* granulovirus matching the catalytic motif of phage NTases and visualised the results.

We aimed to profile substrate specificity of phage and viral NTases, so we modelled[177] the complexes between one of the NTases and pairs of NTPs (we only used ATP, GTP, or UTP, as they are typically utilised by CD-NTases) and 3 ions of Mg^{2+}, which have been reported as cofactors stabilising donor and acceptor NTPs[174]. We visualised the ipTM and pTM scores as heatmaps. We used Pymol to visualise the hydrogen bonds formed between *Erinnyis ello* granulovirus NTase, two molecules of UTP and three ions of Mg^{2+}.

QUANTIFICATION AND STATISTICAL ANALYSIS

The p-values and e-values produced by tools are described in the text with references to original articles.

We used the Mann-Whitney U-test to compare the distributions in Figure 3A, and the Fisher exact test to calculate the odds ratio and p-value in Figure 3B.

We calculated correlation between ipTM scores for phage and viral NTase using Pearson correlation coefficients.